

Computer vision-based smart HVAC control system for university classroom in a subtropical climate

Lan Haifeng^a, Huiying (Cynthia) Hou^{a*}, Zhonghua Gou^b, Man Sing Wong^c, Zhe Wang^d

^a Department of Building Environment and Energy Engineering, The Hong Kong Polytechnic University, Hong Kong, China;

^b School of Urban Design, Wuhan University, Wuhan, China

^c Department of Land Surveying and Geo-Informatics, The Hong Kong Polytechnic University, Hung Hom, Hong Kong, China

^d Department of Civil and Environmental Engineering, The Hong Kong University of Science and Technology, Hong Kong, China

Corresponding author: Huiying (Cynthia) Hou

Email: cynthia.hou@polyu.edu.hk

Abstract: To respond to the increasing demand for a comfortable, productive and energy efficient study environment, the application of artificial intelligence technologies in the smart control of Heating, ventilation, and air conditioning (HVAC) systems plays an increasingly important role. This research uses a classroom, equipped with a traditional central HVAC system, in Hong Kong as a case study to demonstrate an innovative approach for a more intelligent and efficient HVAC system. Through a field investigation (i.e. measurement and questionnaire) and Computational Fluid Dynamics (CFD) simulation, it is found that the number and spatial location of students have a significant impact on their thermal comfort. Applying a computer vision model (YOLOv5) detected dynamic occupant information (variations in student numbers and locations) in a classroom, the SimScale (a cloud-native simulation platform) was then used to estimate the current thermal comfort state (predicted mean vote, PMV) and change in PMV (Δ PMV) of students in the classroom. Furthermore, a fuzzy logic control system is implemented to adjust air temperature and air velocity based on the simulation results. Preliminary scenario analysis has proven the feasibility of the proposed smart HVAC system for classrooms, as well as its ability to provide better quality of thermal comfort with more robust control. This study contributes to the smart and low-carbon retrofitting of university buildings with traditional central HVAC systems, while also serving as a benchmark for the energy-efficient transformation of HVAC systems in other types of indoor spaces.

Keywords: Thermal comfort; University classroom; Smart HVAC system; Computer vision; CFD simulation

Abbreviation	Definition
COVID-19	Coronavirus Disease in 2019
CFD	Computational Fluid Dynamics
HVAC	Heating, Ventilation, and Air Conditioning
k- ω SST	k- ω Shear Stress Transport
mAP50-95	mean Average Precision for Intersection over Union thresholds from 0.50 to 0.95
MPC	Model Predictive Control
PCMs	Personal thermal comfort models
PMV	Predicted Mean Vote
PPD	Predicted Percentage of Dissatisfied
RGB	Red, Green, and Blue
RL	Reinforcement Learning
SD	Standard Deviation
TCS	Thermal Comfort Satisfaction
TSV	Thermal Sensation Vote
YOLOv5	You Only Look Once version 5

1. Introduction

Formal learning spaces, such as lecture theatres and classrooms, should have characteristics that provide a comfortable learning and teaching environment [1][2]. Thermal comfort is a key component in the quality of indoor environments and it needs to be considered in classroom operations [3][4]. Numerous research findings [4][5] indicate that its significance rests in its capacity to foster an environment conducive to students' learning efficiency and health. The significance of thermal comfort has been emphasised even more in the post-COVID-19 pandemic era, urging students and the education sector to prioritise it [3][6][7].

1.1 Challenges in thermal comfort in university classrooms

Compared to other education sectors, such as primary, secondary and high schools, university buildings are more energy intensive [8][9]. The higher energy usage index of university buildings is due to the large number of students in university classrooms, all of whom are adults in the age group 18–30, and the longer hours of use (9am to 10pm). This means that more energy is required to guarantee thermal comfort in the classrooms [2][10][9]. More importantly, uncertainty and randomness introduced by the variability in college students' course participation and seating choices [2][10], compounded further by the shift towards online courses in the aftermath of the COVID-19 pandemic, further confound the situation[11][12]. In addition to this, new post-pandemic mandates from universities regulate maximum room occupancy and advocate for appropriate physical separation between occupants, adding yet another layer of complexity to management of classroom environments. This implies that existing HVAC systems need to be adaptable to

these new conditions and requirements [7][13][14]. To ensure the efficacy of HVAC control solutions, it is essential to consider these evolving dynamics and potential changes in the classroom environment.

Contemporary HVAC systems, predominantly utilized in universities, face several challenges due to their inherent insensitivity to students' mobility and randomness within the classrooms [5][12][15]. Current control measures heavily depend on temperature sensors of the air conditioning system, often resulting in delayed or inaccurate responses [9][16]. Furthermore, the position of the thermostat can substantially affect the performance of control systems and the thermal comfort of occupants. Due to the location of this singular point of measurement, it may not be possible to perceive the precise ramifications of even substantial temperature changes in the environment [17][18][19]. In addition, the prevalent HVAC systems in university classrooms are centralised HVAC systems that use ductwork to distribute cold air throughout the building. Although these systems are highly efficient for large spaces, they frequently result in excessive energy consumption and high operational expenses [20][21]. In a classroom, a common practice is setting the HVAC system to a lower fixed temperature, such as 20-23 degrees Celsius, and leaving it running throughout the day, regardless of the number of occupants in the classroom or the outdoor weather conditions[2][15]. However, the practice can lead to energy wastage and escalated operational costs, while also potentially leading to discomfort due to excessive or fluctuating cold conditions [7][9][15]. Therefore, an updating of HVAC control strategies considering these factors is critical to enhancing efficiency and comfort.

1.2 Objectives of this study

Smart HVAC systems have gained attention due to their potential to maximise energy efficiency and indoor comfort. Recent research has proposed dynamic HVAC operation systems based on computer vision rather than sensors [16][17][23]. By combining cameras with advanced deep learning algorithms, these studies have effectively developed more accurate and dependable occupancy detection systems. The occupancy data collected by these systems was then used to dynamically regulate HVAC operational parameters, such as temperature and ventilation. The results of these studies indicate an exceptional detection accuracy of over 90%, resulting in energy saving of up to 30%.

In addition to computer vision, predictive control techniques such as reinforcement learning (RL) and model predictive control (MPC) are increasingly used in HVAC control to optimise energy consumption and indoor comfort based on predicted information [24][25]. These techniques allow the HVAC system to adapt to changing conditions and learn from previous experiences, thereby enhancing its overall performance. Numerous researchers have also studied the occupancy detection, CFD simulation, and control systems for intelligent HVAC operations over the past decade [14][21][26]. The development of sophisticated occupancy detection algorithms, more accurate and faster CFD simulations, and control systems able to adapt promptly and accurately to changes has advanced, despite the fact that real-time adjustment and practical implementation still face obstacles.

Previous research has confirmed the effectiveness and energy efficiency of intelligent HVAC control systems in maintaining thermal comfort. Typically, these studies have been conducted in the context of spaces with fewer occupants, such as chambers, private living room, and office spaces. However, the development and implementation of intelligent

HVAC systems specifically tailored to the unique requirements of university classrooms remains relatively understudied [2][27][28]. In response to the growing demand for intellectuallisation and humanisation of HVAC systems for university students, the purpose of this study is to investigate the effect of occupant randomness on thermal comfort in university classrooms and to investigate a holistic framework for updating HVAC systems so that they can adapt to the dynamic nature of university classrooms. Although still in the nascent stage of developing its theoretical framework, and facing challenges in practical application, this study endeavours to probe into the potential of energy-efficient and intelligent transformation of university buildings. It advocates for the creation of a low-carbon, smart, and sustainable campus and urban environment, which is essential for the future of educational institutions and society. To address this, a typical Hong Kong university classroom with a conventional ducted central HVAC system has been chosen as a case study. Several research issues guide this investigation.

(1) How does the different number of students and spatial locations in the classroom affect the thermal environment of the classroom, and what is the difference in the thermal sensation of the students?

(2) How does the classroom's physical thermal environment change over time, and how long does it take for the environment to be stabilised?

(3) How to dynamically detect and monitor the number and location of students in the classroom, and how to develop a comprehensive framework so that the temperature and velocity of the HVAC system can be adjusted according to the classroom's dynamic situation?

The paper is organised as follows. Section 1 introduces the background, objectives and questions posed in this study. In Section 2, we review and summarise the relevant research into indoor thermal environmental control. Section 3 describes the steps and methods required to develop a smart HVAC system. Section 4 presents the field study and simulation results and analyses the performance of the proposed smart HVAC system. Section 5 discusses the innovations and limitations, and proposes future research directions. Section 6 summarises the major findings and implications of this paper.

2. Related works

2.1 Thermal environment control for indoor spaces

There are three commonly used methods for the automatic control of an indoor thermal environment, namely controls based on indoor air temperature, PMV, and thermal sensation prediction.

2.1.1 Temperature settings-based control

An HVAC control system based on temperature settings refers to the use of temperature sensors to achieve the automatic adjustment of the thermal comfort of an indoor space. This method was recognised by Kaya [29] in the 1980s and the indoor condition is roughly within the thermal comfort range recommended by ASHRAE, and energy consumption can be reduced. However, the thermal comfort of an indoor environment is not fully reflected by temperature [30][27][31]. Relying solely on temperature sensors to control HVAC systems can be problematic because it is difficult to detect these changes in a timely manner. As a result, this method of control may not provide a consistently high quality indoor thermal comfort environment [32][33].

2.1.2 PMV-based control

In the 1970s, Fanger [34] put forward the PMV prediction model through statistical analysis. It took into account air temperature, humidity, velocity, average radiation temperature, clothing thermal resistance and human metabolic rate. After this model was proposed, it was used by a large number of researchers and is currently one of the most commonly used thermal comfort models. In recent years, there have been studies that propose HVAC control systems based on the Predicted Mean Vote (PMV) as a measure of indoor thermal comfort. These studies have shown that such systems are effective in meeting thermal comfort requirements and saving energy [22][32][35][36]. For example, Freire [36] found that using fuzzy predictive control systems in HVAC, with PMV as a measure of thermal comfort, resulted in energy savings. Maher et al. [32] proposed a fuzzy logic control system based on PMV, which saved about 10% more energy and was more practical to implement. Although the indoor thermal comfort control method based on PMV has high practicability and accuracy under steady-state conditions, it is relatively difficult to obtain measurable PMV. A way to apply it to more complex and dynamic thermal environments still needs further exploration.

2.1.3 Thermal sensation prediction-based control

This method uses personal thermal sensation prediction models (PCMs), which incorporate dynamic environmental and personal data, to predict human comfort levels, and then adjusts the indoor environment accordingly [31][37]-[38]. For example, Chaudhuri et al. [37] used peripheral skin temperature and gradient features from a single body location to evaluate the thermal state, while Farhan et al. [39] predicted human comfort in real-time using environmental conditions, and psychological, and physiological features. These methods can provide high levels of thermal comfort for individuals, but collecting sufficient data to train and test the models can be challenging, especially in public spaces with many occupants.

To sum up, HVAC control systems relying solely on temperature sensors can result in longer and less reliable adjustment cycles. Control methods based on individual thermal sensation prediction are less suitable in shared spaces such as classrooms, as they put too much emphasis on individual comfort and can be less generalisable. On the other hand, PMV-based thermal comfort control systems are more practical and suitable for use in public areas.

2.2 Dynamic thermal comfort control

Detecting the dynamic situation of students in a classroom is important for improving the thermal comfort and energy efficiency of the air conditioning system. In the literature, there has been innumerable work on human detection using a variety of techniques, such as RGB cameras, thermal arrays, and thermal cameras [40][41]. For example, a head detection method was proposed by Oosterhout et al. [42], based on range data from stereo cameras for counting people. The method is robust and provides high accuracy, ranging from 90-95% for different scenarios. Similarly, Beltran et al. [41] used a combination of thermal sensors and PIR (passive infrared) sensors to accurately estimate occupancy.

At the same time, some research studies have combined occupant detection with thermal comfort control [16][43]. Muhammad et al. [43] designed and implemented an occupancy-predictive HVAC control system that used a Raspberry Pi-3, video processing, and machine learning, to recognise real-time occupancy, predict occupancy patterns, and

control HVAC operations. Mahmoud et al. [16] used a computer vision system to identify an occupant's actions, which were then translated into a predicted mean vote (PMV) thermal comfort index. The integration of the PMV thermal comfort index and action recognition system allowed for the adaptive control of an occupant's thermal comfort without the need for a sensor on the occupant at all times.

Despite the fact that analogous research has been conducted in office conference rooms, university classrooms exhibit distinct characteristics. The differences lie in the patterns of occupancy, spatial layouts, occupant behaviour, and building characteristic. Typically, university classrooms are characterised by a high population density, fluctuating enrolment, and limited individual environmental control. Given these differences, it is clear that thermal comfort solutions designed for offices may not be as effective in university classrooms. Thermal comfort in university classrooms necessitates a dedicated study and customised solutions due to their unique challenges [27][31][44]. This paper aims to address these limitations by proposing a new classroom thermal comfort control method framework that combines thermal comfort numerical simulation technology and machine vision technology to achieve high quality thermal comfort with lower energy consumption.

3. Methodology

The research framework of this study is outlined in Figure 1, which includes three major processes. The study begins by conducting a field investigation to gather data on student perception and satisfaction of the thermal environment in a classroom, with variable numbers of students and their location distribution. These data were collected through a combination of subjective questionnaire surveys and objective measurements of environmental conditions. With this data, the thermal comfort of the classroom could be assessed, and the differences in students' perceptions of the classroom thermal environment can be identified as well. Next, numerical simulation was employed to model the thermal environment of the classroom. Based on the actual 3D model of the classroom and real-world conditions, boundary conditions for the simulation were set. The PMV (Predicted Mean Vote) index, which is derived from field measurements taken at various points within the classroom, serves as a comparator for the PMV values obtained from simulation results. After many meticulous adjustments, the simulation provides a faithful representation of the actual thermodynamic processes taking place in the classroom. Then, this calibrated model was then used to understand why students may be dissatisfied with the thermal environment, as well as to inform adjustments to the HVAC system. Finally, the study proposes a smart HVAC control system for university classrooms that integrates computer vision, fuzzy logic and numerical simulation technology. Specifically, by simulating the results of PMV and ΔPMV to infer the specific regulation strategies of temperature and velocity of the HVAC system. Further details can be found in the following subsection.

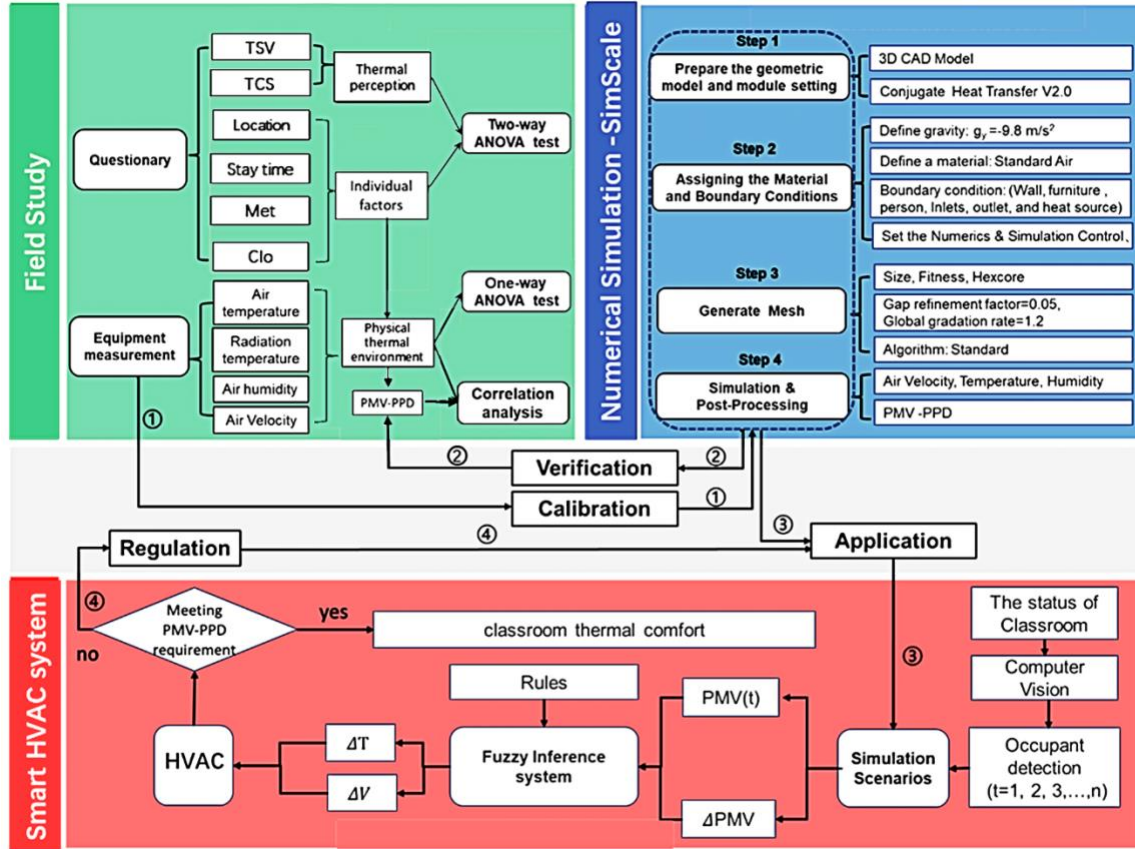


Figure 1. The research framework

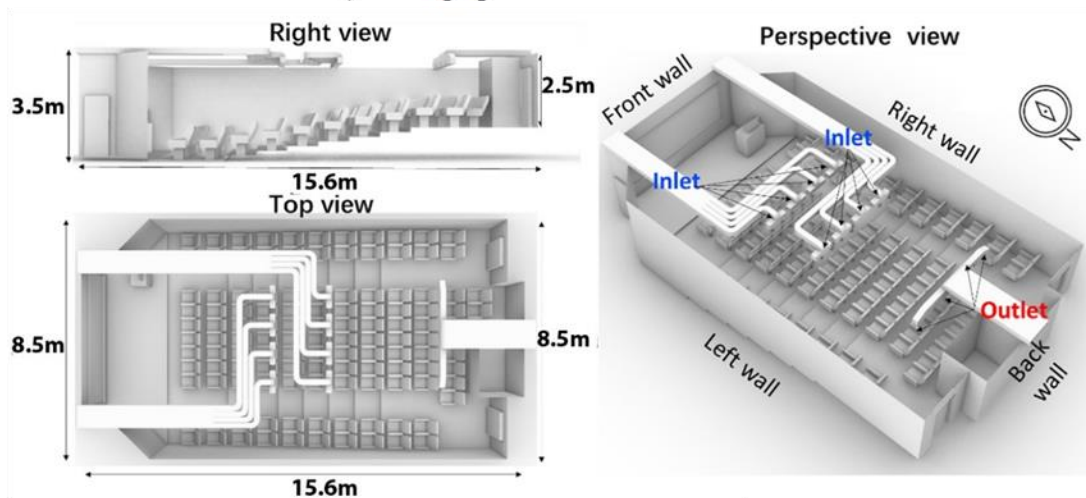
3.1 Field study

3.1.1 Study case

The lecture theatre chosen for this study is located at the Hong Kong Polytechnic University, Hong Kong, China and is a typical example of a lecture theatre. The classroom is equipped with individual controllers for a central HVAC system. These controllers can modify the air temperature and velocity of the corresponding outlets. The room has a total capacity of 112 seats, arranged in 12 rows. The dimensions of the lecture theatre are 15.8 x 8.5 m, with a total of 7 steps, each measuring 0.15 m in height. The south wall is an internal wall with a height of 3.5 m, while the north wall is an external wall measuring 2.5 m in height and is connected to the corridor. The west and east walls are both internal walls without windows. The lecture hall is equipped with 8 air inlets, positioned at a height of 3.5 m. These inlets are divided into three distinct groups, with the purpose of providing targeted air flow to specific areas of the room. The two inlets located on the left side of the lecture hall primarily supply air to the front and back sections on the left side of the room. Similarly, the two inlets on the right side of the room primarily supply air to the front and back sections on the right side of the room. Additionally, the four air inlets located in the middle of the room primarily supply air flow to the front and back sections of the centre of the room. The four return air outlets are located near the back wall, at a height of 3.5 m. Figure 1 shows the specific layout of the classroom.



a). Photograph of the lecture theatre



b) 3D model of the lecture theatre


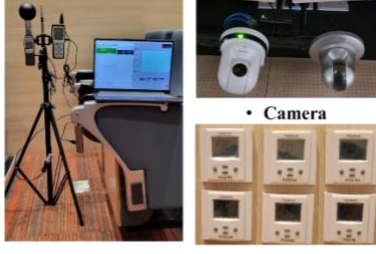



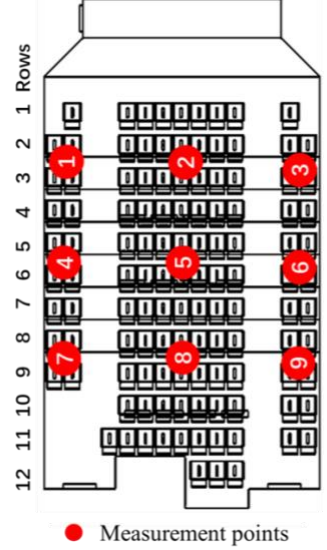
Figure 2. The study area

3.1.2 Field measurement and questionnaire

To assess indoor thermal comfort, a comprehensive evaluation was conducted by gathering data through a combination of instrument measurements and questionnaire surveys. The measurements were taken from 6:30pm to 9:30pm on Wednesdays, from September 7 to September 28. The measurements and questionnaires for this investigation were collected simultaneously at the same time and date. This specific time period was selected for three main reasons: (1) September is the warmest months of the academic year for students in Hong Kong, when they have classes and spend significant time on campus. (2) The 6:30pm to 9:30pm. time frame for the measurements was determined through negotiations with campus administration and students. This collaborative decision-making process indicates that careful consideration was given to selecting a time that would have minimal disruption to classroom learning. (3) The time slot for data collection was also a strategic decision intended to eradicate the effects of solar radiation, particularly on the rear wall of the classroom, which may be directly exposed to sunlight. Solar radiation during the day is an

uncontrollable variable in the research. The study's simulations did not consider solar radiation. To mitigate its potential influence on the results, measurements were strategically planned to be conducted after sunset. This decision aimed at enabling a more unbiased comparison between simulation outcomes and actual measurement data. The environmental variables that influence thermal comfort, such as air temperature, humidity, velocity, and radiation temperature, were measured using specialised instruments. The locations of these measurements, and the details of the measuring instruments used, are summarised in Table 1. The questionnaire survey was divided into three sections. The first section collected data on parameters related to thermal comfort, such as the clothing worn and level of activity, which were used to calculate clothing thermal resistance and metabolism. The second section aimed to gather information about the location chosen by the students and the time spent in the classroom. The third section focused on investigating the students' subjective perception and satisfaction with the thermal environment.

Table 1. Equipment and measurement

Equipment	Range and accuracy	Products images	Placement and distribution
Heat index WBGT meter model 8778	Air temperance: 0~50°C (±0.3°C) Globe temperature: 0~80°C (±0.5°C) WBGT temperature: 0~50°C (±0.6°C) Relative humidity: 0~100% (±2%)		 • Camera
Xima Hot-Film Anemometer AR866A	Air velocity: 0~30m/s (±1% or ± 0.1m/s) Wind temperature: 0~45°C (±1°C)		• Thermal and velocity Meter • HVAC controller
Valuecon Digital Thermostat RDF300.02	Temperature Range: -10 to 60 °C 3-speed fan Current Rating: 2A Material : Copper		
Panasonic WV-SC384	720P ,30 FPS Focal length: 4.7 mm ~ 84.6 mm Scanning Area: 4.8 mm (H) x 3.6 mm (V)		 • Measurement points

3.1.3 Thermal comfort indicator

The evaluation and measurement methods used for assessing the indoor thermal environment adhere to the standards ISO7730 [4] and ASHRAE 55 [45]. These standards utilise the PMV-PPD (predicted mean vote and predicted percentage dissatisfied) thermal comfort evaluation index proposed by Professor P.O. Fanger of Denmark [46]-[47]. The PMV-PPD index comprehensively considers environmental factors and human factors, including individual activities, clothing, air temperature, air relative humidity, air velocity, and average radiation temperature. The specific formula for this index is represented by equations (1-5).

$$PMV = \left((0.303e^{-0.036M} + 0.028) \{ M - W - 3.05 \times 10^{-5} [5733 - 6.99(M - W) - P_a] - 0.42[M - W - 58.15] - 1.7 \times 10^{-5} M(5867 - P_a) - 0.0014M(34 - t_a) - 3.96 \times 10^{-8} f_{cl} [(t_{cl} + 273)^4 - (t_r + 273)^4] - f_{cl} h_c (t_{cl} - t_a) \} \right) \quad (1)$$

$$PPD = 100 - 95 \exp[-(0.03353 PMV^4 + 0.2179 PMV^2)] \quad (2)$$

$$f_{cl} = \begin{cases} 1.00 + 1.290I_{cl}, & \text{if } I_{cl} \leq 0.078 \\ 1.05 + 0.645I_{cl}, & \text{if } I_{cl} > 0.078 \end{cases} \quad (3)$$

$$t_{cl} = 35.7 - 0.028(M - W) - I_{cl} \{ 3.96 \times 10^{-8} f_{cl} [(t_{cl} + 273)^4 - (t_r + 273)^4] + f_{cl} h_c (t_{cl} - t_a) \} \quad (4)$$

$$h_c = \begin{cases} 2.38(t_{cl} - t_a)^{0.25}, & \text{if } 2.38(t_{cl} - t_a)^{0.25} > 1.21\sqrt{V_a} \\ 1.21\sqrt{V_a}, & \text{if } 2.38(t_{cl} - t_a)^{0.25} < 1.21\sqrt{V_a} \end{cases} \quad (5)$$

where M is the metabolic rate (W/m^2); W is the external work (W/m^2); P_a is the partial water vapour pressure; t_a is the indoor mean temperature ($^{\circ}C$), t_r is the indoor mean radiant temperature ($^{\circ}C$); f_{cl} is the ratio of the body's surface area when fully clothed to the body's surface area when nude, I_{cl} is clothing heat resistance ($m^2 \cdot K/W$); t_{cl} is the surface temperature of clothing ($^{\circ}C$); h_c is the convective heat transfer coefficient between the occupant and the environment $W/(m^2 \cdot K)$; and V_a is air velocity (m/s).

3.2 Computational fluid dynamics numerical simulation

Computational fluid dynamics (CFD) numerical simulation can provide valuable insights into thermal comfort and help assess the level of dissatisfaction in buildings. By using computational models to simulate the flow of air and heat within a building, CFD can help identify potential problem areas and provide information that can be used to make improvements and enhance thermal comfort [28]. However, the major barriers that prevent HVAC design engineers and architects from using this technology is the lack of CFD expertise, the high upfront cost associated with the software license and access to computational resources. This study used SimScale, a cloud-native simulation platform, to simulate the indoor thermal environment of the classroom. The SimScale platform offers a convenient and effective solution for testing, validating, and improving HVAC designs using CFD, heat transfer, and thermal analysis. With SimScale, users can take advantage of advanced simulation capabilities that are not available on traditional, locally-installed computer systems. Furthermore, simulation on the SimScale platform is characterized by its speed, precision, ease of use, and intuitive nature, making it a highly accessible and user-friendly solution[48].

3.2.1 Turbulence model

In CFD numerical simulation, the Reynolds-averaged Navier-Stokes (RANS) method is employed to solve the turbulence problems in a more feasible and effective manner [49][50]. The flow of air in the classroom was regarded as being a steady, incompressible, low-velocity turbulent flow. This study adopts the k - ω shear stress transport (k - ω SST) turbulence model to model the turbulent effects appearing in a CFD simulation. The k - ω SST model is a hybrid of the k - ω and the k - ϵ models and is widely used in the industry due to its high accuracy and cost-effectiveness [51]. The governing equations of the k - ω SST model are presented in detail (5-11).

Equation (5) is the turbulence kinetic energy equation:

$$\frac{\partial k}{\partial t} + U_j \frac{\partial k}{\partial x_j} = P_k - \beta^* k \omega + \frac{\partial}{\partial t} [(\nu + \sigma_k \nu_T) \frac{\partial k}{\partial x_j}] \quad (5)$$

The specific dissipation rate is (6):

$$\frac{\partial \omega}{\partial t} + U_j \frac{\partial \omega}{\partial x_j} = \alpha S^2 - \beta \omega^2 + \frac{\partial}{\partial x_j} [(v + \sigma_\omega v_T) \frac{\partial \omega}{\partial x_j}] + 2(1 - F_1) \sigma_{\omega 2} \frac{1}{w} \frac{\partial k}{\partial x_i} \frac{\partial \omega}{\partial x_i} \quad (6)$$

The kinematic eddy viscosity equation is (7):

$$v_T = \frac{a_1 k}{\max(a_1 \omega, S F_2)} \quad (7)$$

The auxiliary relations equations are (8-11):

$$P_k = \min(\tau_{ij} \frac{\partial U_j}{\partial x_i}, 10 \beta^* k \omega) \quad (8)$$

$$F1 = \tanh \left\{ \left\{ \min \left[\max \left(\frac{\sqrt{k}}{\beta^* \omega y}, \frac{500 v}{y^2 \omega}, \frac{4 \sigma_{\omega 2} k}{C D_{kw} y^2} \right) \right] \right\}^4 \right\} \quad (9)$$

$$F2 = \tanh \left[\left[\max \left(\frac{2 \sqrt{k}}{\beta^* \omega y}, \frac{500 v}{y^2 \omega} \right) \right]^2 \right] \quad (10)$$

$$C D_{kw} = \max(2 \rho \sigma_{\omega 2} \frac{1}{w} \frac{\partial k}{\partial x_i} \frac{\partial \omega}{\partial x_i}, 10^{-10}) \quad (11)$$

3.2.2 Boundary condition setting

The classroom in this study was designed with no windows, and the airflow was entirely provided by the ventilation system. The front, left, and right walls, floor, and furniture of the classroom were considered to be internal walls and assigned adiabatic boundary conditions, as they faced the interior of the building and were expected to have similar temperature conditions as the neighbouring rooms. The initial boundary temperature of the inner walls was set to around 23.5°C and was characterised as opaque, with an emissivity of 0.9. The ceiling of the classroom was equipped with 72 LED lights, each with a power of 10 W, evenly distributed across an area of 132.6 m², and an additional heat flux of 5.43 W/m² was added to the ceiling. The back wall was designated as an external wall, due to the significant temperature difference between the inside and outside environments, leading to heat transfer. The ambient temperature was set to 33°C and the initial boundary temperature of the back wall was 23.5°C, with a thickness of 0.18 m and a contact conductance of 0.35 W/(K·m²). The boundary conditions are detailed in Table 3. In addition, the heat generated by a single student while seated quietly is estimated to be 75 watts, based on the typical resting metabolic rate of an adult [52], which covers the energy needed for basic physiological functions, such as temperature regulation, breathing, and circulation. Figure 3 depicts the distribution of these inlets, outlets, probe sites, and the 3D geometry of an individual person. The PMV-PPD thermal comfort index can be calculated utilising CFD to simulate environmental conditions and integrating personal parameters such as clothing and metabolic rate. For the PMV-PPD calculation, the metabolic rate is set to 1.0 (sedentary state) and the apparel thermal resistance is set to 0.6 (typical summer attire) in accordance with ASHRAE Standard 55 [45], which applies to healthy adult men and women.

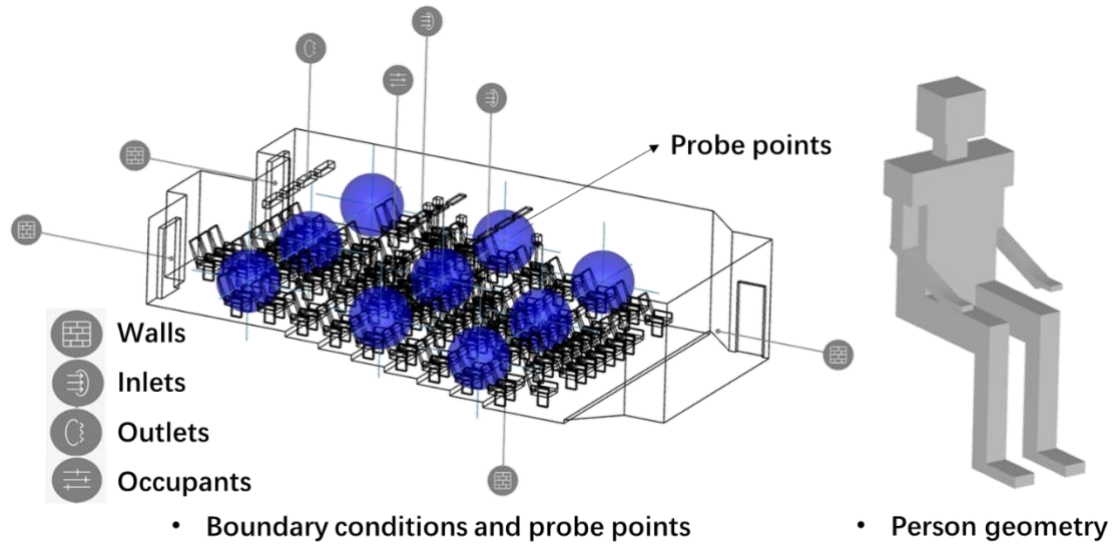


Figure 3. The diagram of boundary conditions, probe points and person geometry

Table 2. The inlet and outlet settings

Boundary conditions	Velocity type	Velocity (m/s)	Length (m)	Width (m)	Temperature (°C)
Left Inlet × 2	Mean value	Front =1.0	0.8	0.3	21.5
		Left =1.0			
		Down=0.5			
Centre Inlet ×4	Mean value	Front =1.5	0.8	0.3	21.5
		Left/right =0.0			
		Down=0.5			
Right Inlet × 2	Mean value	Front =1.0	0.8	0.3	21.5
		Right =1.0			
		Down=0.5			
Outlet1 ×4	Pressure outlet	Gauge pressure =0.0 Pa	0.6	0.4	-

3.2.3 Mesh generation

A finer mesh results in a higher resolution of small geometric features, but it also increases the computation time and memory requirements of the simulation. A trade-off between the fineness of the mesh and the computation time must be made. After extensive experimentation with different precision levels and mesh sizes, and with valuable advice from the SimScale technical team, a standard setting was adopted in this study. Based on the 3D model of the classroom and the boundary conditions, a three-dimensional unstructured mesh using tetrahedral or hexahedral elements was generated. An expanded exposition of the experiments, specifically those associated with mesh generation and precision tests, can be found in the supplementary material. Table S1 details the parameters and results of the mesh generation process. The chosen mesh for this study was of fineness 5, exhibiting an overall mesh quality of 0.257, comfortably situated within the acceptable bounds of 0.035 to 1.0. Simulations conducted at this mesh fineness level presented a similarity about 90% when compared with results obtained from the mesh of highest

quality (fineness=9) in this study. Thus, the quality of the selected mesh was deemed adequately satisfactory to fulfil the requirements for this study, considering both acceptable error margins and computational resources. Figure 4 provides a visual depiction of the generated mesh, covering the entire scope of the classroom.

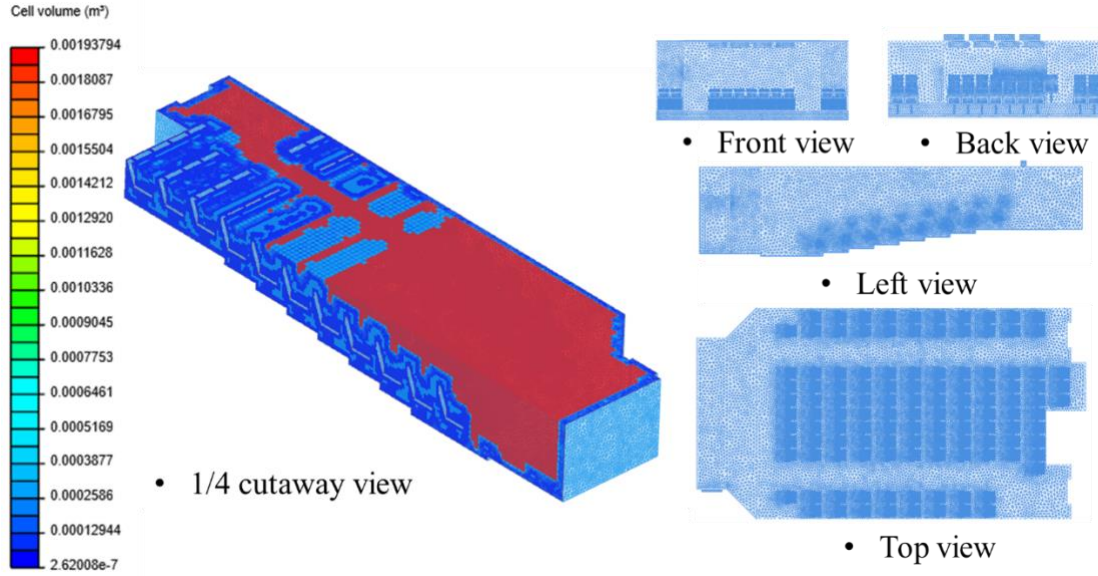


Figure 4. The generated mesh

3.3 Machine vision-based smart HVAC

This study presents a smart HVAC thermal control method that combines computer vision technology, a CFD numerical simulation cloud platform (SimScale), and a fuzzy logic control system. It was designed to improve the thermal comfort of an indoor environment by automatically adjusting the temperature and velocity of the inlets, based on the number and distribution of occupants present in the classroom. The machine vision model was used to automatically detect the number and distribution of students in the classroom. The numerical simulation cloud platform (SimScale) was then utilised to simulate the thermal comfort environment (PMV and Δ PMV) in the classroom under the current conditions. The simulation results were then used as inputs for the fuzzy logic control system, which issued corresponding commands to adjust the temperature and velocity of the inlets, thereby optimising the indoor thermal comfort environment. The flowchart of the system is illustrated in Figure 5, which depicts a schematic diagram of the smart thermal control system.

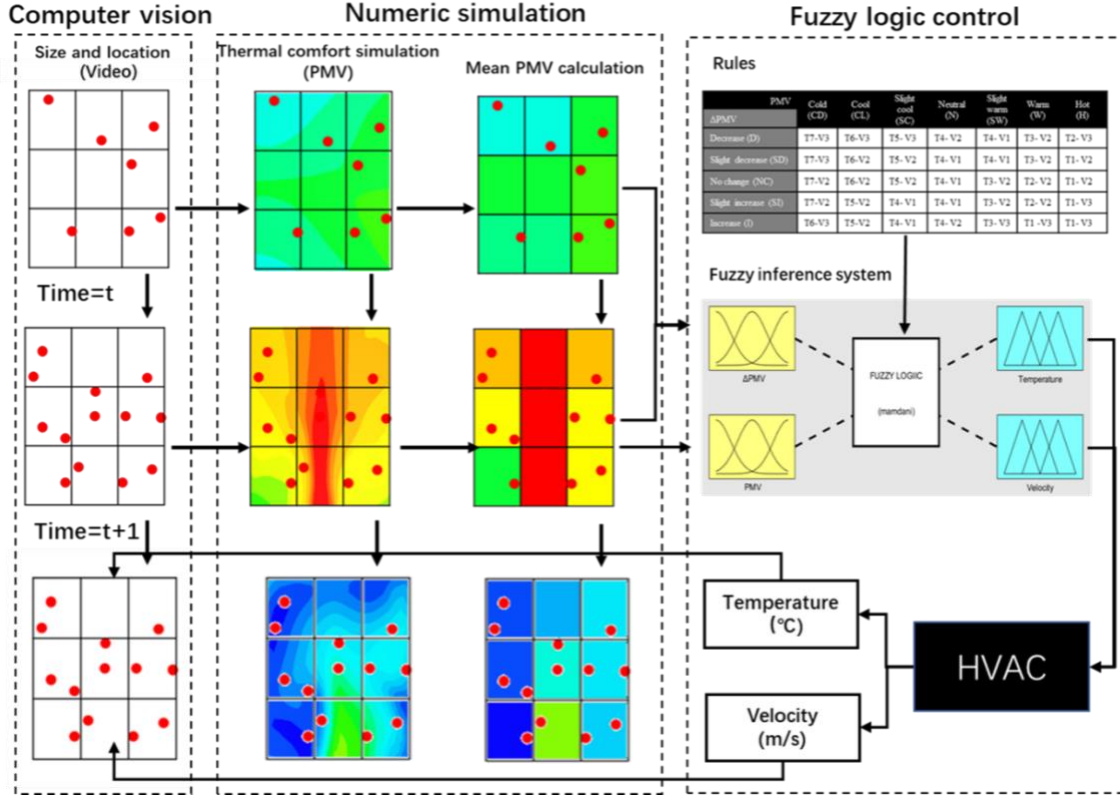


Figure 5. The schematic diagram of the smart HVAC control system

3.3.1 Computer vision-based occupant detection system.

This paper adopted the YOLOv5 (You Only Look Once version 5) training model. YOLOv5 is a real-time object detection model that uses a single convolutional neural network (CNN) to identify objects within an image. The network structure of YOLOv5 is a classic one-stage structure, which is divided into input, backbone, neck and head. The main principle of YOLOv5 is to divide the input image into a grid of cells and then predict the bounding boxes and class probabilities for each cell [53]. One key advantage of YOLOv5 is its speed, as it can process images at a faster rate than many other object detection models. Additionally, YOLOv5 has a lightweight architecture and requires very few computational resources, which allows it to be run on resource-constrained devices.

Among the YOLOv5 Series models, the YOLOv5s model with the shortest network, the fastest speed, and the lowest average accuracy was chosen in this research because the identification of students' heads in a classroom is rather straightforward, necessitating a simple network rather than a more sophisticated one, to improve the detection speed. The dataset for training and testing in YOLOv5s is the Classroom Monitoring Dataset from the Kaggle platform [54]. The dataset consists of 2,000 photos (1,600 for training set and 400 for test set) of students in the classroom and corresponding labels.

Figure 6 shows an example of using this model to identify the number of student and their spatial location in a classroom. More details and the complete code can be found at the GitHub link: <http://github.com/laifenglan/YoloV5-for-students-detection>. Throughout the training process of the YOLOv5s model for detecting students in a classroom, both the training and validation loss gradually decreased. It is worth noting that the validation loss remained slightly higher than the training loss, indicating that the model

was not overfitting to the training data. Specifically, after 100 epochs, the training loss stabilized with a value of 0.22, while the validation loss remained at 0.49. The precision and recall of the model were calculated as 88.1% and 86.5%, respectively, through the verification of the test set. The model also achieved an mAP50 of 92.3%, indicating that it accurately identified objects of interest with high confidence. Furthermore, the model achieved an mAP50-95 of 77.4%, demonstrating good performance across a range of confidence thresholds from 0.5 to 0.95.

In summary, the gradual decrease in training and validation loss during the epoch process indicates that the model was able to effectively learn from the training data. The YOLOv5s model is able to effectively detect students in a classroom setting, with high accuracy and good performance across a range of confidence thresholds.

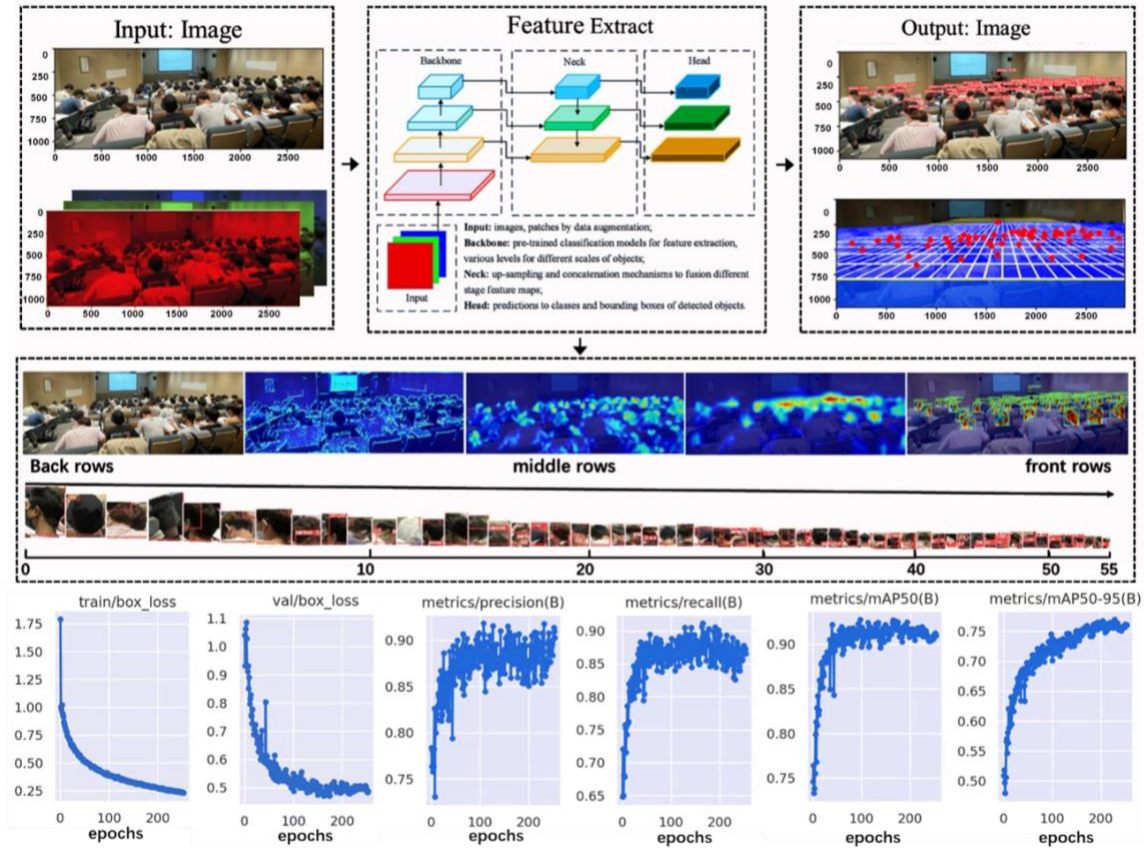


Figure 6. Detection of the number and distribution of students in a classroom

3.3.2 Fuzzy logic based thermal control systems

Fuzzy Logic utilises degrees of membership, rather than binary values of true or false, to provide added flexibility to artificial intelligence control systems. This means that, rather than simply being true or false, a variable can be assigned a value between 0 and 1 that reflects the degree to which it belongs to a certain category. Fuzzy Logic is able to adjust its control strategy in real-time, based on the current conditions, making it highly adaptable and responsive to changes in the environment. This allows for a more precise and efficient control of the indoor environment, which can result in improved comfort, energy savings, and reduced emissions. This study employed the MATLAB fuzzy control toolbox to design a fuzzy controller. With this tool, complex operations, such as fuzzification, inference, and

defuzzification, are not necessary. By simply setting the appropriate parameters, such as input and output variables and rules, a fuzzy control system can be quickly established and easily modified.

The fuzzy logic controller uses the PMV and ΔPMV index, derived from the numerical simulation, as the input variables. ΔPMV is the difference between the current PMV and the previous PMV. PMV and ΔPMV is considered to be the major and minor parameter controlling the inlets' temperature and velocity, respectively. PMV ranges from too cold (-3~-2) to too warm (2~3), with 7 fuzzy subsets. ΔPMV ranges from a large decrease (-1~-0.5) to a large increase (0.5~1.0), with 5 fuzzy subsets. Temperature and velocity are the 'out' variables, with temperature ranging from T1 (18~20 °C) to T7 (29~31 °C), with 7 fuzzy subsets, and velocity ranging from V1 (0~2 m/s) to V3 (3~4 m/s), with 3 fuzzy subsets. The gear setting of temperature and velocity regulation is basically consistent with the existing air conditioning system. The fuzzy sets for the input and output variables are included in Table 3 and Figure 7.

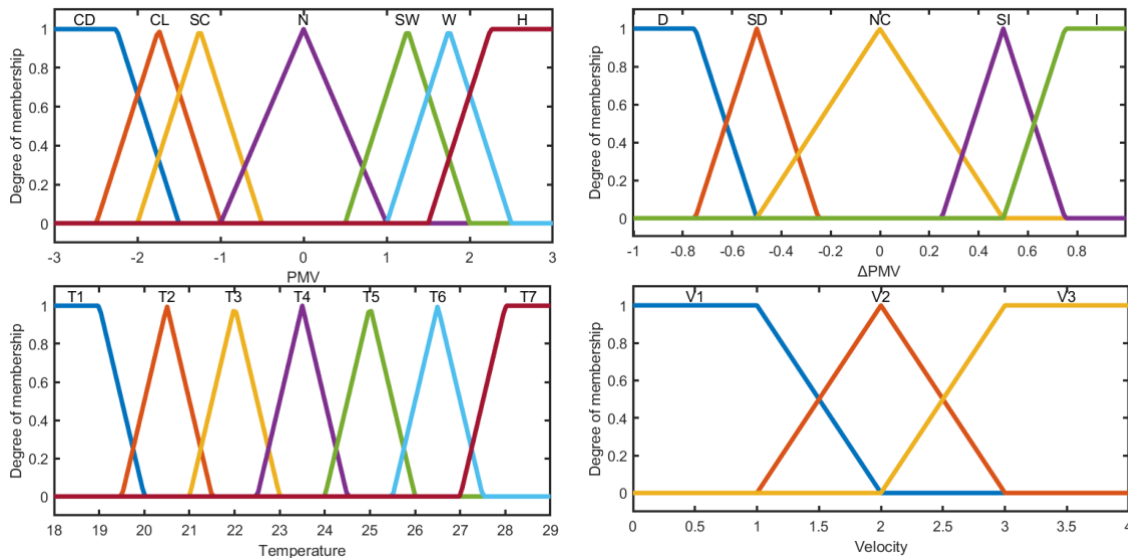


Figure 7. The membership of input and output variables

Table 3. Fuzzy logical control in terms of input and output.

Input				Output			
PMV		ΔPMV		Temperature (°C)		Velocity (m/s)	
Terms	Sets	Terms	Sets	Terms	Set	Terms	Sets
Cold (CD)	-3~-2	Decrease(D)	-1.0~-0.5	T1	18~20	V1	0~2
Cool (CL)	-2.5~-1.0	Slight decrease (SD)	-0.75~-0.25	T2	19.5~21.5		
Slightly cool (SC)	-2.0~-0.5	No change (NC)	-0.5~0.5	T3	21~23		
Neutral (N)	-1~1			T4	22.5~24.5	V2	1~3
Slightly warm (SW)	0.5~2			T5	24~26		
Warm (W)	1.0~2.5	Slight increase (SI)	0.3~0.5	T6	25.5~27.5	V3	2~4
Hot (H)	2~3	Increase (I)	0.5~1.0	T7	27~29		

The PMV and Δ PMV indices are used as inputs for the fuzzy controller to control the temperature and velocity based on pre-determined rules. The relationship between the input and output variables can be seen in Figure 8 and the specific rules can be found in Table 4. The fundamental concept behind these rules is that when the PMV and Δ PMV values are high, a lower temperature and higher velocity are chosen, and when the PMV and Δ PMV values are low, a higher temperature and higher velocity are chosen. When the PMV is close to the comfortable range, the temperature is adjusted to a moderate level and the velocity of air is adjusted to control changes in the Δ PMV.

Table 4. Rules of fuzzy temperature control system based on PMV and Δ PMV inputs

Δ PMV	PMV	Cold (CD)	Cool (CL)	Slightly cool (SC)	Neutral (N)	Slightly warm (SW)	Warm (W)	Hot (H)
Decrease (D)	T7-V3	T6-V3	T5- V2	T4- V2	T4- V1	T3- V2	T2- V3	
Slight decrease (SD)	T7-V3	T6-V2	T5- V2	T4- V1	T4- V1	T3- V2	T2- V3	
No change (NC)	T7-V3	T6-V2	T4- V2	T4- V1	T4- V2	T2- V2	T1- V3	
Slight increase (SI)	T6-V3	T5-V2	T4- V1	T4- V1	T3- V2	T2- V2	T1- V3	
Increase (I)	T6-V3	T5-V2	T4- V1	T4- V2	T3- V2	T2- V3	T1- V3	

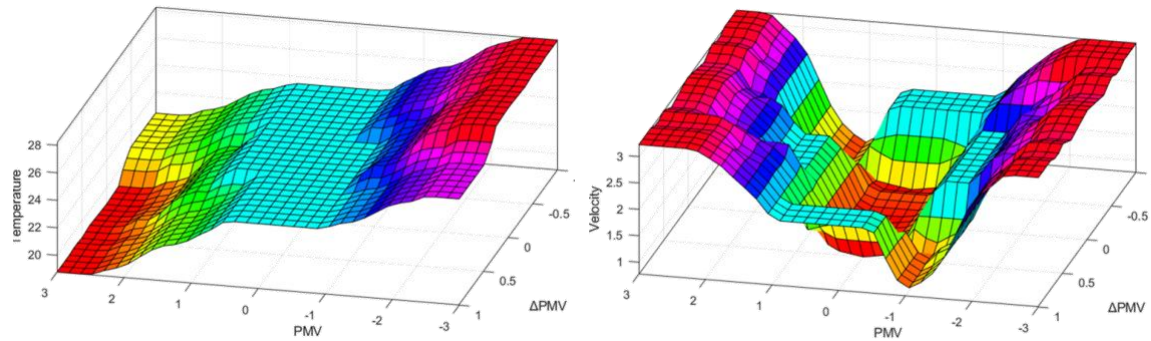


Figure 8. Relationship between input variables and output variables

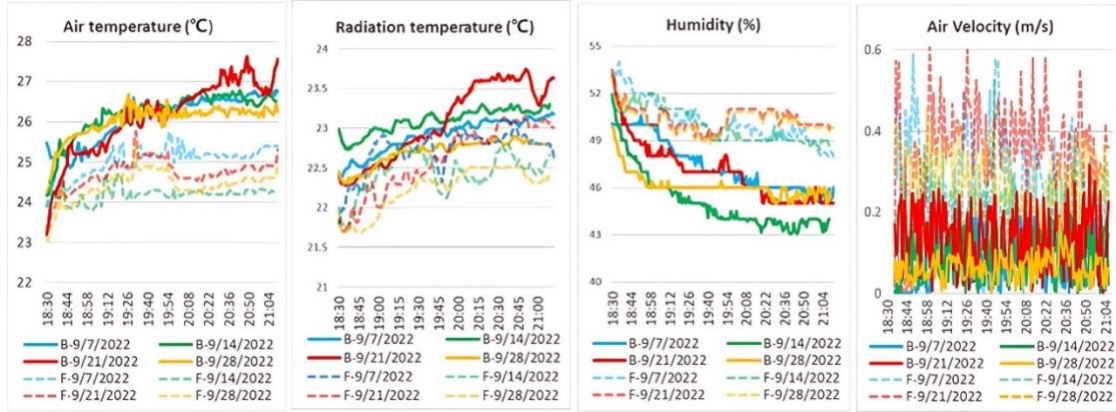
4. Results

4.1 Measurements and questionnaires

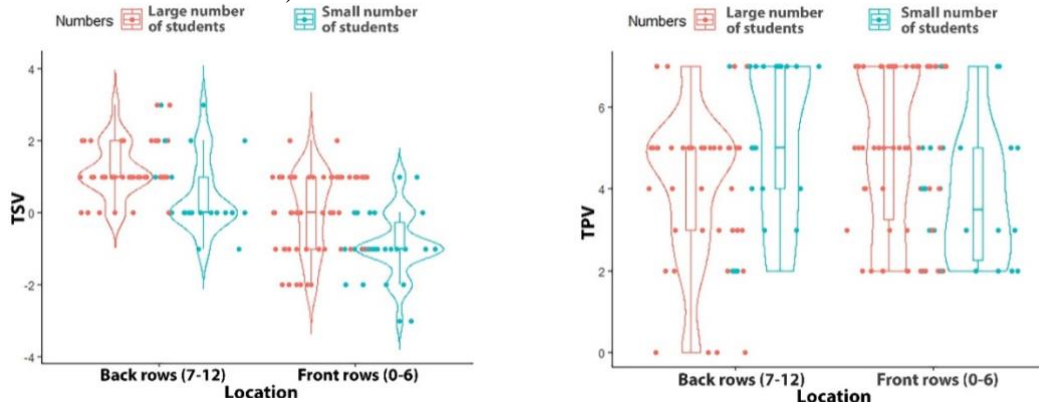
The results of this study demonstrate that there are clear variations in the thermal environment between the front and back rows of the classroom. The data collected from the instruments shows that after about an hour, the air temperature and radiation temperature increased while the air humidity decreased and reached a steady state. Compared to the front row, the back row of a classroom has a higher temperature, higher radiation temperature, and lower humidity and velocity. The pairwise comparison using the Games-Howell method (as seen in Table 5) found statistically significant differences between the front and back rows, in terms of temperature (1.53°C higher in the back row), radiation temperature (0.435°C higher in the back row), humidity (3.74% lower in the back row), and velocity (0.17 m/s lower in the back row).

Furthermore, a two-way ANOVA test was used to investigate the differences of thermal sensation vote (TSV) and thermal comfort satisfaction (TCS) among the students (Table 6 and Figure 9-b). In general, the average TSV of students in the back row is 1.228 higher than that of students in the front row, with statistical significance ($P < 0.01$). The

average TSV in the classroom with fewer students is 0.8085 lower than that in the classroom with more students, and the difference was statistically significant ($P < 0.01$). The average TCS of students in the back rows is 0.5489 lower than that of students in the front rows, with statistical significance ($P < 0.01$). The average TCS in the classroom with fewer students is 0.6997 higher than that in the classroom with more students, and the difference was statistically significant ($P < 0.01$).



a) Measurement of thermal environment



b) Students' objective perception of thermal environment

Figure 9. Description and analysis of the field study data

Table 5. Description measurement data and one-way ANOVA test

Sensor Location		Back rows				Front rows				P -value
Date		9/7	9/14	9/21	9/28	9/7	9/14	9/21/	9/28	
Counts		160	160	160	160	160	160	160	160	640
Temperature	Mean	26.10	26.21	26.13	26.03	25.01	24.19	24.71	24.41	1.53 (1.47~1.59) 0.0013 ***
	SD	0.56	0.55	0.89	0.41	0.36	0.17	0.36	0.36	
	Min	24.85	24.17	23.20	24.25	23.90	23.80	23.35	23.05	
	Max	26.80	26.80	27.62	26.67	25.74	24.73	25.75	25.45	
Radiation temperature	Mean	22.9	23.1	23.07	22.7	22.72	22.44	22.6	22.23	0.435 (0.397~0.435) 0.0025 ***
	SD	0.21	0.15	0.48	0.16	0.25	0.25	0.43	0.21	
	Min	22.36	22.73	22.28	22.31	21.80	21.73	21.70	22.36	
	Max	23.17	23.30	23.74	22.90	23.01	22.80	23.17	23.17	
Humidity	Mean	47.43	45.10	47.02	46.11	50.26	49.93	50.44	50.24	-3.74

	SD	1.86	1.81	0.79	1.36	1.09	0.71	0.71	1.86	(-3.57~-3.90)
	Min	45.08	43.08	45.00	45.00	48.00	48.42	49.00	48.80	0.0042
	Max	50.58	51.92	53.17	49.92	54.00	52.00	53.50	53.30	****
Velocity	Mean	0.27	0.17	0.35	0.27	0.08	0.09	0.14	0.06	-0.17
	SD	0.12	0.09	0.13	0.08	0.06	0.06	0.08	0.03	(-0.22~-0.12)
	Min	0.025	0.09	0.12	0.00	0.00	0.01	0.02	0.01	0.0006
	Max	0.59	0.52	0.60	0.46	0.19	0.20	0.31	0.18	***

Note: a. SD are mean (standard variation). b. p-values were obtained from the one-way ANOVA tests (Games-Howell); c. p-values less than 0.01 are in bold.

Table 6. Description of TSV and TSS and two-way ANOVA test

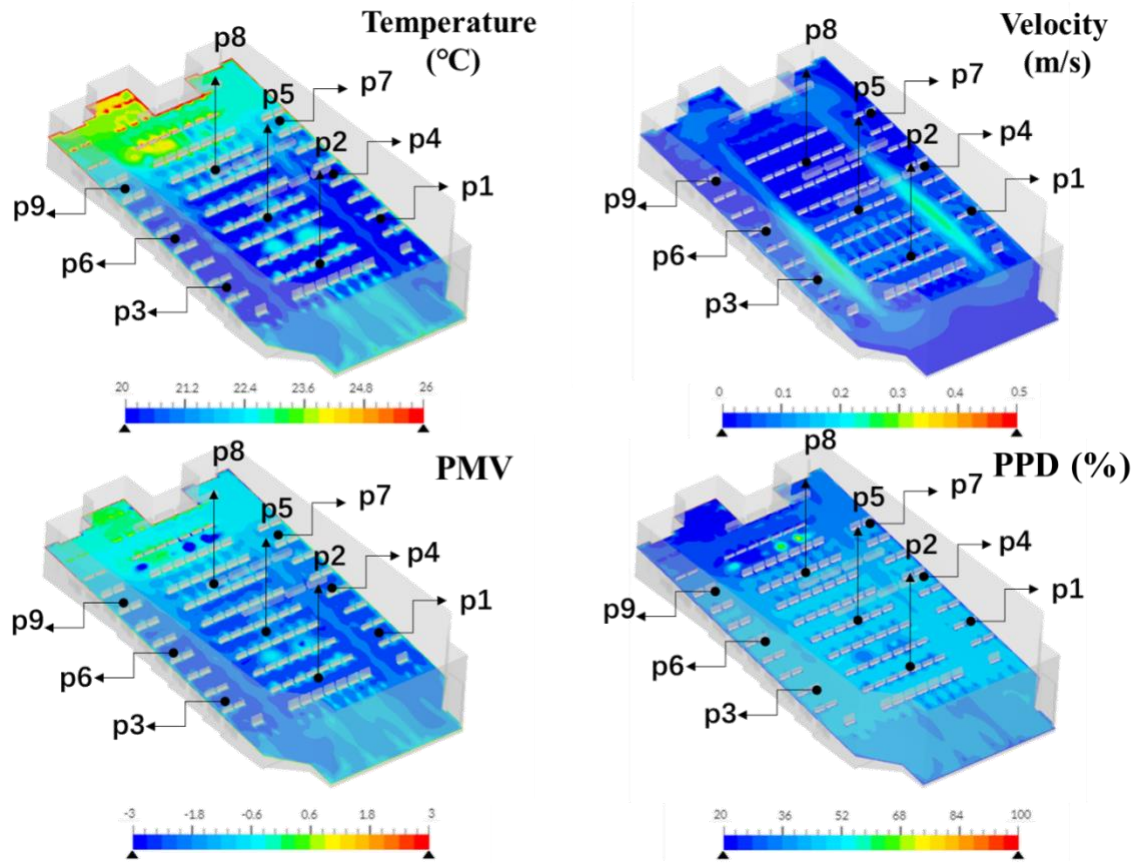
Questionnaire	Groups	Small number of students			Large number of students		
		Mean (SD)	Min-Max	skew	Mean (SD)	Min-Max	skew
TSV	Front rows	-0.88 (0.91)	-3~1	0.09	0.04 (1.12)	-2~2	-0.39
	Back rows	0.48 (1.03)	-1~3	0.84	1.20 (0.76)	-1~3	0.36
TCS	Front rows	3.81 (1.63)	2-7	-0.57	5.00 (1.94)	2-7	-0.33
	Back rows	5.19(1.97)	2_7	-0.40	4.00 (1.89)	0_7	-0.62
TSV	Two- way	Groups		Difference	Lower	Upper	P-value
	ANOVA	Small number –Large number		-0.8085	-1.1520	-0.4649	0.000
	test	Front rows- Back rows		-1.2288	-1.5557	-0.9020	0.000
TCS	Two- way	Small number –Large number		0.5489	-0.5392	0.8414	0.0067
	ANOVA	Front rows- Back rows		0.6997	-0.4571	0.8566	0.0054
	test						

Note: a. SD are mean (standard variation). b. p-values were obtained from the two-way ANOVA tests (Games-Howell); c. p-values less than 0.01 are in bold.

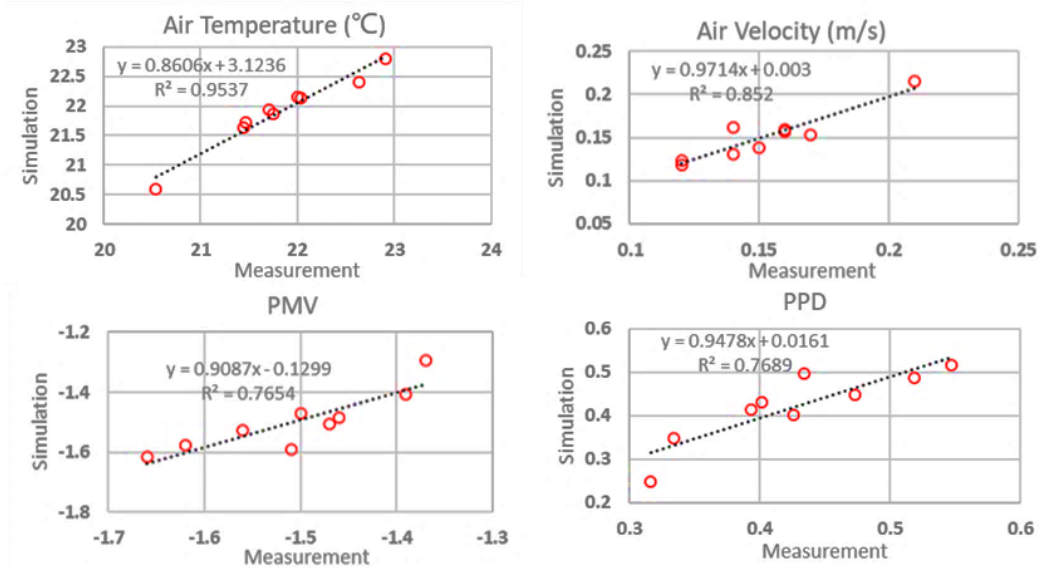
4.2 Validity of simulation

The measurements and simulation are both based on the situation when the classroom is empty, for the purposes of validating and calibrating the numerical simulation. In the simulation, the size of the room, furniture, doors and air vent are as consistent as they are in the physical environment. The results are shown in Figure 10(a), where the mean temperature at points 1 to 9 is between 20.4°C and 22.9°C, at a height of 1.1 m. It is noticeable that the temperatures of the front rows are a little bit lower than the back rows in the classroom. The mean velocity of points 1 to 9 is between 0.12 and 0.21 m/s, while the velocity in the aisle is relatively large, approximately 0.15~0.21 m/s. The predicted mean vote (PMV) of the points from 1 to 9 is between -1.8 and -1.2. The predicted percentage of dissatisfied (PPD) (at points 1 to 9) is between 25% and 55%. Generally, the PMV and PPD values indicate that the thermal environment of the classroom is less comfortable because it makes students feel cool or cold.

The validity of the numerical simulations is confirmed by comparing them with the measured results. The simulated and measured results are compared at the 9 points in Figure 10b, which shows a similar trend in temperature, velocity, PMV, and PPD. The R^2 between the measured and simulated results is relatively high, ranging from 0.76-0.95, indicating a high degree of consistency. However, it should be noted that the simulation results are slightly cooler than the actual measurements due to the unaccounted for heat sources, such as projectors and computers. The numerical simulation results have been validated and shown to be accurate.



a) The result of simulation at the cross-section plane at height $y=1.1$ m.



b) Comparison of the measurements with the simulations

Figure 10. Validation of simulation results

4.3 Performance of smart HVAC

The calibrated CFD model was utilised to evaluate the performance of the smart HVAC control system through scenario analysis. Three distinct scenarios were devised for this purpose: Scenario 1 had fewer than 10% of the seats occupied by students; Scenario 2 had over 25% of the seats occupied by students; and Scenario 3 had more than 50% of the seats occupied by students. The detailed analysis of each of these three scenarios is presented in Figure 5.

Scenario 1:

This scenario examines the performance of the smart HVAC control system in a classroom with low student occupancy. Using computer vision, the model detects that only 9 students are present and mainly located in the centre left of the room. The original setting is shown as iteration 0 and it results in a slightly cold classroom environment with a PMV range of -1.4 to 0.5. This means that most of the front row space is uncomfortable, causing students to feel cool or cold. In contrast, the back row space is within the thermal comfort zone with a PMV range of -0.5 to 0.5. However, the model continues to adjust the thermal comfort in iterations 1 to 3, by implementing commands from the designed fuzzy logic system. The results show that the PMV of the classroom space gradually improves, becoming more comfortable, and the gap between the front and back row temperatures decreases.

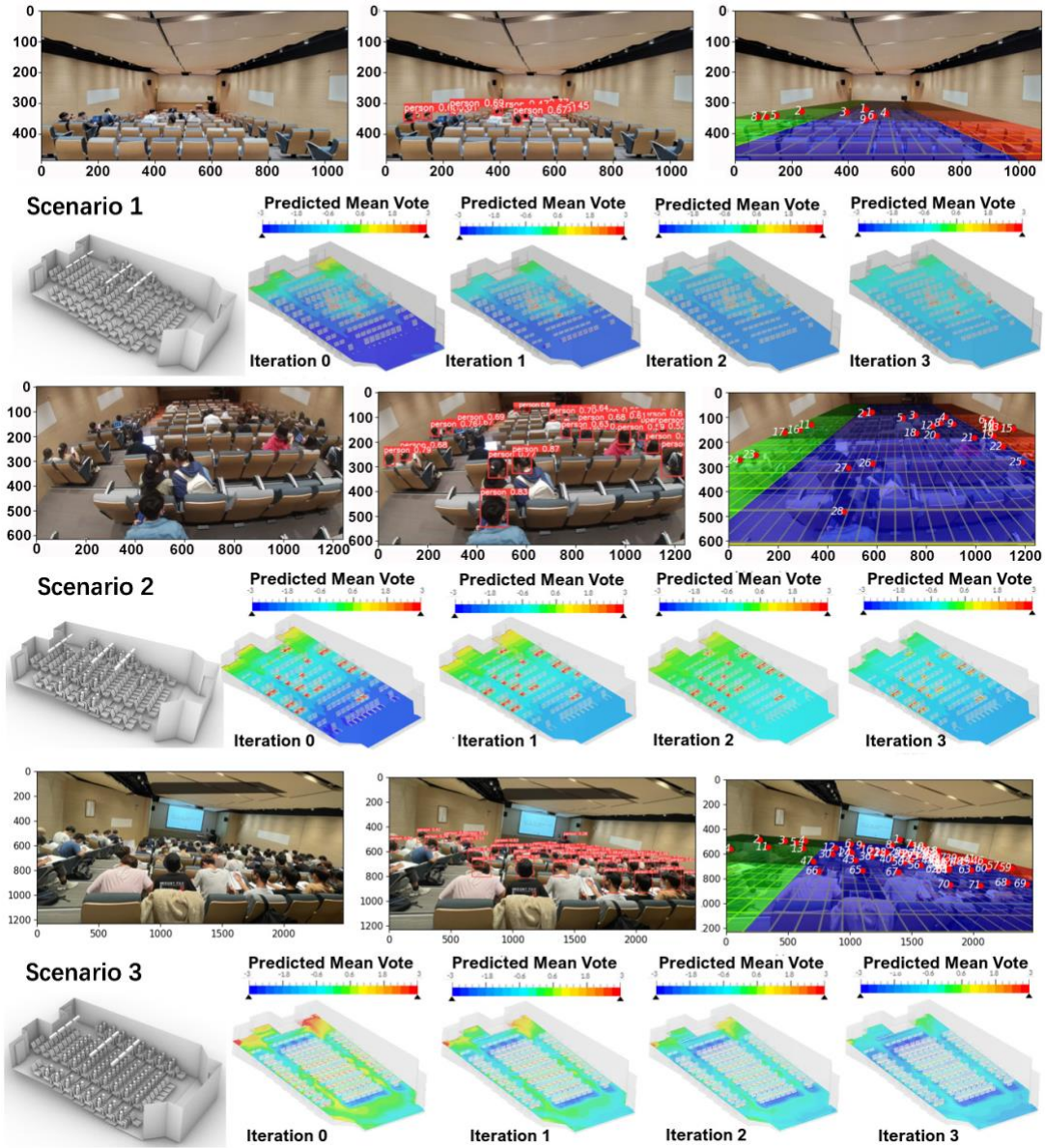
Scenario 2:

In this scenario, the machine vision detection system recognises the presence of 28 students in the classroom. The initial thermal comfort results of the numerical simulation, as shown in iteration 0, indicate that the average PMV of the classroom falls between -1.2 and 1.4. Although the middle row of the classroom is in the thermal comfort zone (PMV values ranging from -0.5 to 0.5), there is a noticeable difference in temperature between the front and back rows, with the front row being cooler and the back row being warmer. After multiple iterations, the gap between the front and back rows slowly decreases and the PMV values for both the front and back rows slowly move closer to the thermal comfort zone.

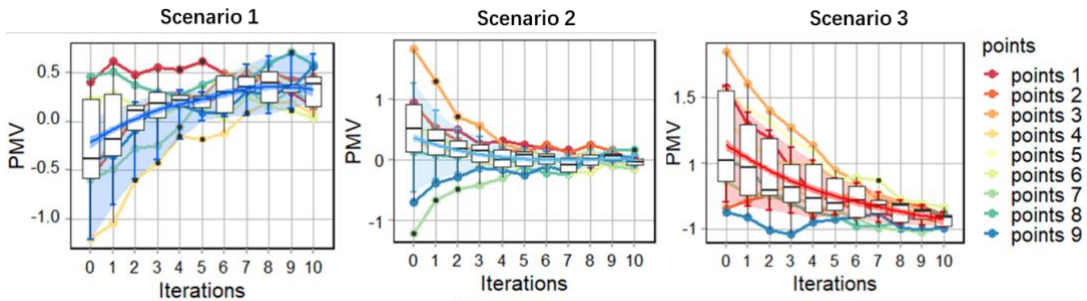
Scenario 3:

This scenario features a classroom with 71 students detected by the machine vision system. The results of the initial thermal comfort simulation, shown in iteration 0, reveal an overall PMV ranging from -0.6 to 1.8. At this point, the front portion of the classroom falls within the thermal comfort zone ($-0.5 \leq \text{PMV} \leq 0.5$), while the back portion is uncomfortably warm ($\text{PMV} > 0.5$). Through the subsequent iterations 1 to 3, the PMV of the back row is gradually adjusted towards the thermal comfort zone, resulting in a closing of the gap between the front and back rows.

The performance of the smart HVAC control system under the three scenarios is demonstrated in more detail in Figure 11b. As the number of iterations increases, the PMV of the classroom tends to approach the thermal comfort zone, making the hot spaces progressively cooler and the cold spaces progressively warmer until they are close to the comfort zone. The thermal comfort zone remains relatively unchanged. Basically, after three iterations, the thermal comfort of the classroom reaches a stable state, with PMV fluctuations generally remaining within the comfort range. This suggests that the thermal comfort of the classroom can be effectively maintained within just three adjustments from the smart HVAC system.



a) Examples of testing Smart HVAC performance in three scenarios



b) The performance of Smart HVAC under three scenarios based on simulation

Figure 11. Scenario analysis of the performance of Smart HVAC control system

5. Discussion

5.1 Human factor impact on classroom thermal comfort

This study examines the impact of student numbers and their location on thermal comfort in air-conditioned classrooms. The results indicate that changes in the distribution and number of students have a marked effect on the thermal comfort of the classroom and the comfort levels of the students [2][4][55]. [22,56]. This study found that, as the number of students increases, so does the total amount of metabolic heat generated, resulting in a rise in room temperature [22,56]. This effect is most pronounced in the back of the classroom, where restricted airflow and proximity to exterior walls can cause heat to accumulate and produce warmer conditions. Second, the distribution of students can also affect the surrounding temperature. If students congregate in one area of the room, this localised density can result in an increase in temperature due to increased metabolic heat. On the contrary, areas with fewer students may remain cooler as a result of less metabolic heat. The variability in student numbers and distribution can result in spatial differences in classroom temperatures and thermal comfort levels.

This study also revealed that the heat exchange between human body heat and the classroom's thermal environment does not occur immediately. In a scenario in which the classroom temperature is set to 22 degrees with low velocity, it takes approximately one hour for the thermal environment to stabilise from a state of near-emptiness to near-full occupancy. The stabilization time of HVAC systems in different spaces, such as bedrooms, offices, and classrooms, can vary based on a variety of factors. These encompass the room size, the HVAC system's capacity, the number of occupants, potential heat sources, and other variables. When the HVAC system is properly designed and sized for a space, smaller rooms with fewer occupants, such as bedrooms or offices, can typically achieve HVAC stabilisation within the relatively short time frame[57][58]. On the other hand, larger rooms like classrooms, which have larger size and more occupants, may take more time to stabilize. However, when equipped with an appropriately sized HVAC system, these larger rooms can also aim for comparable stabilization times. Our study underscores the necessity for a dynamic adjustment mechanism, one that not only strives to minimise stabilisation time but also accounts for both the current and evolving states of thermal comfort to maintain a consistently comfortable classroom temperature.

5.2 The advantage of the smart HVAC control approach

This study presents a novel method for monitoring and adjusting the thermal comfort of classrooms by combining several cutting-edge technologies: computer vision, CFD simulation, and Fuzzy Logic control. Computer vision technology involves teaching machines to "see" and interpret visual data from the actual world. In this context, it is confirmed that the yolov5 model can precisely track the number and location of students in a classroom. CFD is an effective method for comprehending and enhancing thermal comfort. Using a cloud-based simulation platform can significantly reduce the complexity of these simulations. Then, fuzzy logic is used to adjust the control strategy of the HVAC system. It allows for a flexible and adaptable approach to sustaining thermal comfort, allowing for classroom adjustments.

Compared to previous studies [43][59][16], one of the key advantages of this method is that it is more accurate to dynamically monitor the number and location of students by using computer vision technology. In addition, the use of CFD simulations

generates a comprehensive thermal profile of the classroom. This profile, which consists of the distribution of temperature, humidity, and velocity fields, is created without the need for a large number of physical sensors. Also, the investigation approach of this study is a comprehensive framework for collecting and accumulating coupled occupant distribution and CFD simulation data for future research. Furthermore, the fuzz logic control system considers both the current thermal comfort (PMV) and changes in thermal comfort (ΔPMV) to maintain a consistently agreeable thermal environment within the classroom. Moreover, the proposed smart HVAC control system is cost-effective. Compared to the cost of updating or replacing an HVAC system and adding various types of sensors, our proposed investigation mechanism is to utilise the existing infrastructure and augment it with high-precision monitoring equipment. This is considered to be a more cost-effective option.

5.3 The potential solution for practical application

The proposed system has been proved to have the potential of enhancing thermal comfort and decreasing HVAC energy consumption. However, its implementation in actual contexts presents challenges. For the practical implementation of the intelligent HVAC control system, it would be necessary to collect a substantial quantity of historical data and develop robust algorithms and hardware infrastructure. In particular, the proposed method integrates a wide-angle camera, a microcontroller (such as Raspberry Pi), and an infrared transmitter module. The camera in this configuration is capable of detecting variations in classroom occupancy during real-time operation. For example, it can detect a change from 10 to 11 individuals or larger adjustments, such as 10 to 15 individuals. The microcontroller makes decisions based on information gathered from past experiences. If fluctuations in classroom occupancy between 10 and 15 students are grouped into a single category, no additional adjustment may be required. In contrast, if these fluctuations are divided into multiple categories, each may require a distinct adjustment. The function of the microcontroller is not to perform CFD simulations, but rather image data processing. It retrieves the required accumulated data, executes the appropriate algorithm, and transmits infrared commands to the HVAC system controller. As a result, the system does not require a robust computational capacity, making it a practical and effective solution.

It is essential to note that these classifications and modifications will be established following the clustering of massive quantities of data and the establishment of reinforcement learning. Although collecting data and conducting simulations for a variety of scenarios can be difficult and time-consuming, it is a necessary step to enhance the research's relevance to the real world.

5.4 Limitation

The current study principally evaluated the impact of student numbers and location on thermal comfort and energy consumption; a more comprehensive evaluation should consider other factors, such as weather, climate, building characteristics, occupant behaviour, and personal factors like gender, age, and body mass index (BMI) [60]-[61]. This study focuses primarily on human heat sources, and the accuracy of simulation results could be improved by accounting for additional heat sources in the environmental model. Moreover, this study was conducted at night in order to intentionally avoid the potential influence of solar radiation on the results. However, in real-world applications, considering the impact of solar radiation is essential. Solar radiation can significantly affect thermal comfort and energy consumption in a building. Thus, in order to make the model more

applicable and generalizable to real-world scenarios (which would invariably include daylight hours where solar radiation would have an impact), it will be necessary to incorporate the effects of solar radiation into the model in future work.

In addition, it is also important to note that the numerical simulation for thermal comfort still requires a substantial amount of time, approximately 30 to 60 minutes per iteration, which impedes real-time control of HVAC systems. The use of higher performance computers or cloud computing technology can greatly shorten the time needed for the numerical simulation [48]. More promisingly, once a large number of pre-simulated numerical models have accumulated, a numerical simulation process is not required, i.e. the HVAC system directly responds to the actual classroom situation [28][62].

New technologies continue to emerge and improve the comfort, energy efficiency, and sustainability of indoor environments. By using machine learning technology, HVAC systems can continuously improve their performance and adapt to changes in the indoor environment [63]. A more intelligent HVAC system can be trained with techniques such as reinforcement learning, which allows the HVAC system to learn from past experiences and make more effective and efficient decisions [24][25].

While the research in this paper remains at a relatively fundamental stage, it serves as a valuable beginning and case study for the development of energy-efficient solutions in education settings. This study could be further transferred to other learning space for better energy efficiency management. By persistently investigating various learning spaces on campuses, such as interactive classrooms, libraries, and labs, a more sustainable and energy-efficient environment can be established for students and staff. Furthermore, as research and data accumulation increase, they will prove essential for the intelligent transformation of HVAC systems in public buildings, ultimately promoting a more energy-efficient and eco-friendly future.

6. Conclusion

This study is an exploration of the intelligent transformation of HVAC systems in university classrooms. It aims to manage the trade-off between indoor environment quality and HVAC energy consumption. This paper identified the typical thermal environment issues in university classrooms through a field study and numerical simulation. A framework for smart HVAC system control by combining machine vision and numerical simulation technology is proposed. Although this method is not mature, it demonstrates energy saving potential and provides a reference point for later studies. The major findings are as follows.

The number and distribution of students in the classroom significantly affect the air temperature, radiation temperature, air humidity and velocity in the classroom. The physical thermal environment of the classroom is dynamic and requires about one hour to stabilise.

Differences in the physical thermal environment in the classroom can actually be perceived by students, and can be reflected by the objective indicators, such as thermal sensation, comfort, and satisfaction vote.

A CFD numerical simulation model can accurately predict the distribution of thermal comfort in the classroom, after proper calibration through selecting a suitable turbulence model, setting accurate boundary conditions, and generating appropriate mesh sizes.

The YOLOv5 model demonstrated exceptional performance in the detection of students in a real-time classroom setting. Despite having limited training data and

computational resources, the model was still able to achieve a high degree of accuracy and efficiency in detecting the number and spatial distribution of students in the classroom.

Theoretically, the smart HVAC system for classrooms, based on the combination of computer vision and CFD numerical simulation, is feasible and promising. Generally, a classroom with a higher quality of thermal environment can be created in an efficient and effective way.

Acknowledgements

The authors appreciate the kind support and cooperation of the Hong Kong Polytechnic University, who granted permission to conduct data measurements and surveys in the classroom. The authors gratefully acknowledge the SimScale platform for providing an educational version license and access, as well as offering technical support. The authors acknowledge the original code of YOLOv5 and datasets provided by Ultralytics and the Kaggle platform. It is important to note that all of the videos and images used in this paper were obtained with permission from the students and no personal information or privacy was violated.

This study was supported by grants from the Hong Kong Polytechnic University: Start-up Fund for New Recruits (Project ID: P0040305). M.S. Wong thanks the funding support from the General Research Fund (Grant No. 15609421), and the Collaborative Research Fund (Grant No. C5062-21GF) from the Research Grants Council, Hong Kong, China.

References

- [1] A. Martinez-Molina, P. Boarin, I. Tort-Ausina, J.L. Vivancos, Post-occupancy evaluation of a historic primary school in Spain: Comparing PMV, TSV and PD for teachers' and pupils' thermal comfort, *Build. Environ.* 117 (2017) 248–259. <https://doi.org/10.1016/J.BUILDENV.2017.03.010>.
- [2] M.K. Singh, R. Ooka, H.B. Rijal, S. Kumar, A. Kumar, S. Mahapatra, Progress in thermal comfort studies in classrooms over last 50 years and way forward, *Energy Build.* 188–189 (2019) 149–174. <https://doi.org/10.1016/J.ENBUILD.2019.01.051>.
- [3] A.K. Mishra, M.T.H. Derks, L. Kooi, M.G.L.C. Loomans, H.S.M. Kort, Analysing thermal comfort perception of students through the class hour, during heating season, in a university classroom, *Build. Environ.* 125 (2017) 464–474. <https://doi.org/10.1016/J.BUILDENV.2017.09.016>.
- [4] M. Puteh, M.H. Ibrahim, M. Adnan, C.N. Che'Ahmad, N.M. Noh, Thermal Comfort in Classroom: Constraints and Issues, *Procedia - Soc. Behav. Sci.* 46 (2012) 1834–1838. <https://doi.org/10.1016/J.SBSPRO.2012.05.388>.
- [5] C. Ramírez-Dolores, L.A. Lugo-Ramírez, B.A. Hernández-Cortaza, G. Alcalá, J. Lara-Valdés, J. Andaverde, Dataset on thermal comfort, perceived stress, and anxiety in university students under confinement due to COVID-19 in a hot and humid region of Mexico, *Data Br.* 41 (2022) 107996. <https://doi.org/10.1016/J.DIB.2022.107996>.
- [6] P. Barrett, F. Davies, Y. Zhang, L. Barrett, The impact of classroom design on pupils' learning: Final results of a holistic, multi-level analysis, *Build. Environ.* 89 (2015) 118–133. <https://doi.org/10.1016/J.BUILDENV.2015.02.013>.

- [7] H. Qian, T. Miao, L. Liu, X. Zheng, D. Luo, Y. Li, Indoor transmission of SARS-CoV-2, *Indoor Air*. 31 (2021) 639–645. <https://doi.org/10.1111/INA.12766>.
- [8] M. Raatikainen, J.P. Skön, K. Leiviskä, M. Kolehmainen, Intelligent analysis of energy consumption in school buildings, *Appl. Energy*. 165 (2016) 416–429. <https://doi.org/10.1016/j.apenergy.2015.12.072>.
- [9] S. Jing, Y. Lei, H. Wang, C. Song, X. Yan, Thermal comfort and energy-saving potential in university classrooms during the heating season, *Energy Build.* 202 (2019) 109390. <https://doi.org/10.1016/J.ENBUILD.2019.109390>.
- [10] L. Dias Pereira, D. Raimondo, S.P. Corgnati, M. Gameiro Da Silva, Energy consumption in schools - A review paper, *Renew. Sustain. Energy Rev.* 40 (2014) 911–922. <https://doi.org/10.1016/j.rser.2014.08.010>.
- [11] M.T. Miranda, P. Romero, V. Valero-Amaro, J.I. Arranz, I. Montero, Ventilation conditions and their influence on thermal comfort in examination classrooms in times of COVID-19. A case study in a Spanish area with Mediterranean climate, *Int. J. Hyg. Environ. Health*. 240 (2022). <https://doi.org/10.1016/J.IJHEH.2021.113910>.
- [12] M. Muñoz-González, M. Luisa Gómez-Jiménez, P.B. Tchounwou, I. Rodríguez-Vidal, A. Martín-Garín, F. González-Quintial, J. Miguel Rico-Martínez, R.J. Hernández-Minguillón, J. Otaegi, Response to the COVID-19 Pandemic in Classrooms at the University of the Basque Country through a User-Informed Natural Ventilation Demonstrator, *Int. J. Environ. Res. Public Heal*. 2022, Vol. 19, Page 14560. 19 (2022) 14560. <https://doi.org/10.3390/IJERPH192114560>.
- [13] T. Pistochini, C. Mande, S. Chakraborty, Modeling impacts of ventilation and filtration methods on energy use and airborne disease transmission in classrooms, *J. Build. Eng.* 57 (2022). https://doi.org/10.1016/J.JOBE.2022.104840/MODELING_IMPACTS_OF_VENTILATION_AND_FILTRATION_METHODS_ON_ENERGY_USE_AND_AIRBORNE_DISEASE_TRANSMISSION_IN_CLASSROOMS.PDF.
- [14] H. Arjmandi, R. Amini, F. khani, M. Fallahpour, Minimizing the respiratory pathogen transmission: Numerical study and multi-objective optimization of ventilation systems in a classroom, *Therm. Sci. Eng. Prog.* 28 (2022). <https://doi.org/10.1016/J.TSEP.2021.101052>.
- [15] S. Barbhuiya, S. Barbhuiya, Thermal comfort and energy consumption in a UK educational building, *Build. Environ.* 68 (2013) 1–11. <https://doi.org/10.1016/J.BUILDENV.2013.06.002>.
- [16] M. Al-Faris, J. Chiverton, D. Ndzi, A.I. Ahmed, Vision Based Dynamic Thermal Comfort Control Using Fuzzy Logic and Deep Learning, *Appl. Sci.* 2021, Vol. 11, Page 4626. 11 (2021) 4626. <https://doi.org/10.3390/APP11104626>.
- [17] A. Correia, L.M. Ferreira, P. Coimbra, P. Moura, A.T. de Almeida, Smart Thermostats for a Campus Microgrid: Demand Control and Improving Air Quality, *Energies*. 15 (2022). <https://doi.org/10.3390/EN15041359>.
- [18] R. Carli, G. Cavone, S. Ben Othman, M. Dotoli, IoT based architecture for model predictive control of HVAC systems in smart buildings, *Sensors (Switzerland)*. 20 (2020). https://doi.org/10.3390/S20030781/SENSORS_20_00781_PDF.PDF.
- [19] H. Stopps, M.F. Touchie, Managing thermal comfort in contemporary high-rise residential buildings: Using smart thermostats and surveys to identify energy

- efficiency and comfort opportunities, *Build. Environ.* 173 (2020) undefined-undefined. <https://doi.org/10.1016/J.BUILDENV.2020.106748>.
- [20] A. Jindal, N. Kumar, J.J.P.C. Rodrigues, A Heuristic-Based Smart HVAC Energy Management Scheme for University Buildings, *IEEE Trans. Ind. Informatics.* 14 (2018) 5074–5086. <https://doi.org/10.1109/TII.2018.2802454>.
- [21] F. Ascione, R.F. De Masi, M. Mastellone, G.P. Vanoli, The design of safe classrooms of educational buildings for facing contagions and transmission of diseases: A novel approach combining audits, calibrated energy models, building performance (BPS) and computational fluid dynamic (CFD) simulations, *Energy Build.* 230 (2021) undefined-undefined. <https://doi.org/10.1016/J.ENBUILD.2020.110533>.
- [22] S.P. Corgnati, M. Filippi, S. Viazzi, Perception of the thermal environment in high school and university classrooms: Subjective preferences and thermal comfort, *Build. Environ.* 42 (2007) 951–959. <https://doi.org/10.1016/J.BUILDENV.2005.10.027>.
- [23] P.W. Tien, S. Wei, J. Calautit, A Computer Vision-Based Occupancy and Equipment Usage Detection Approach for Reducing Building Energy Demand, *Energies* 2021, Vol. 14, Page 156. 14 (2020) 156. <https://doi.org/10.3390/EN14010156>.
- [24] G. Gao, J. Li, Y. Wen, Energy-Efficient Thermal Comfort Control in Smart Buildings via Deep Reinforcement Learning, (2019). <https://doi.org/10.48550/arxiv.1901.04693>.
- [25] J. Brusey, D. Hintea, E. Gaura, N. Beloe, Reinforcement learning-based thermal comfort control for vehicle cabins, *Mechatronics.* 50 (2018) 413–421. <https://doi.org/10.1016/J.MECHATRONICS.2017.04.010>.
- [26] Y.H. Yau, H.S. Toh, B.T. Chew, N.N. Nik Ghazali, A review of human thermal comfort model in predicting human–environment interaction in non-uniform environmental conditions, *J. Therm. Anal. Calorim.* 147 (2022) 14739–14763. <https://doi.org/10.1007/S10973-022-11585-0/TABLES/8>.
- [27] S. Lu, W. Wang, C. Lin, E.C. Hameen, Data-driven simulation of a thermal comfort-based temperature set-point control with ASHRAE RP884, *Build. Environ.* 156 (2019) 137–146. <https://doi.org/10.1016/J.BUILDENV.2019.03.010>.
- [28] G. Tardioli, R. Filho, P. Bernaud, D. Ntimos, An Innovative Modelling Approach Based on Building Physics and Machine Learning for the Prediction of Indoor Thermal Comfort in an Office Building, *Buildings.* 12 (2022). <https://doi.org/10.3390/buildings12040475>.
- [29] A. Kaya, S.J. Alexander, C.S. Chen, S. Raina, Optimum control policies to minimize energy use in HVAC systems, *Ashrae Trans.* (1982).
- [30] L.-R. Jia, Q.-Y. Li, X. Chen, C.-C. Lee, J. Han, Indoor Thermal and Ventilation Indicator on University Students’s Overall Comfort, *Build.* 2022, Vol. 12, Page 1921. 12 (2022) 1921. <https://doi.org/10.3390/BUILDINGS12111921>.
- [31] D. Li, C.C. Menassa, V.R. Kamat, Personalized human comfort in indoor building environments under diverse conditioning modes, *Build. Environ.* 126 (2017) 304–317. <https://doi.org/10.1016/J.BUILDENV.2017.10.004>.

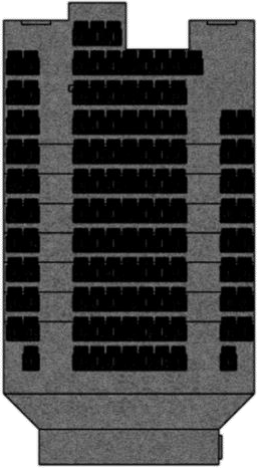
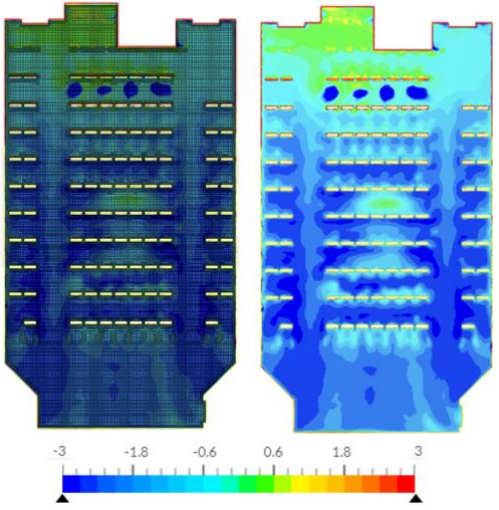
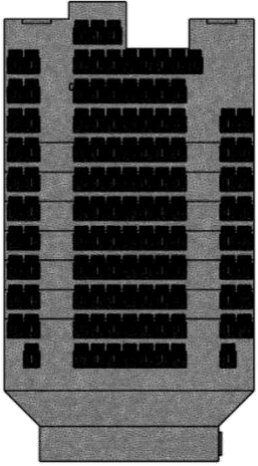
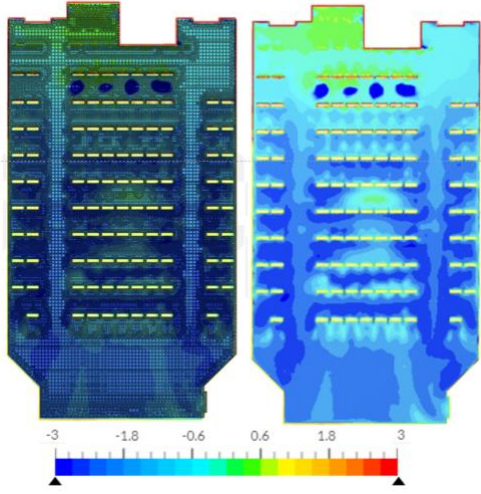
- [32] M. Hamdi, G. Lachiver, A fuzzy control system based on the human sensation of thermal comfort, 1998 IEEE Int. Conf. Fuzzy Syst. Proc. - IEEE World Congr. Comput. Intell. 1 (1998) 487–492. <https://doi.org/10.1109/FUZZY.1998.687534>.
- [33] S. Lu, Dynamic HVAC Operations Based on Occupancy Patterns With Real-Time Vision- Based System, (2017). <https://doi.org/10.1184/R1/6723290.V1>.
- [34] R.J. De Dear, T. Akimoto, E.A. Arens, G. Brager, C. Candido, K.W.D. Cheong, B. Li, N. Nishihara, S.C. Sekhar, S. Tanabe, J. Toftum, H. Zhang, Y. Zhu, Progress in thermal comfort research over the last twenty years, *Indoor Air*. 23 (2013) 442–461. <https://doi.org/10.1111/INA.12046>.
- [35] P.M. Ferreira, S.M. Silva, A.E. Ruano, A.T. Négrier, E.Z.E. Conceição, Neural network PMV estimation for model-based predictive control of HVAC systems, *Proc. Int. Jt. Conf. Neural Networks*. (2012). <https://doi.org/10.1109/IJCNN.2012.6252365>.
- [36] R.Z. Freire, G.H.C. Oliveira, N. Mendes, THERMAL COMFORT BASED PREDICTIVE CONTROLLERS FOR BUILDING HEATING SYSTEMS, *IFAC Proc. Vol. 38* (2005) 113–118. <https://doi.org/10.3182/20050703-6-CZ-1902.01400>.
- [37] T. Chaudhuri, D. Zhai, Y.C. Soh, H. Li, L. Xie, Thermal comfort prediction using normalized skin temperature in a uniform built environment, *Energy Build.* 159 (2018) 426–440. <https://doi.org/10.1016/J.ENBUILD.2017.10.098>.
- [38] J. Kim, Y. Zhou, S. Schiavon, P. Raftery, G. Brager, Personal comfort models: Predicting individuals’ thermal preference using occupant heating and cooling behavior and machine learning, *Build. Environ.* 129 (2018) 96–106. <https://doi.org/10.1016/J.BUILDENV.2017.12.011>.
- [39] A.A. Farhan, K. Pattipati, B. Wang, P. Luh, Predicting individual thermal comfort using machine learning algorithms, *IEEE Int. Conf. Autom. Sci. Eng.* 2015-October (2015) 708–713. <https://doi.org/10.1109/COASE.2015.7294164>.
- [40] D.B. Yang, H.H. González-Baños, L.J. Guibas, Counting people in crowds with a real-time network of simple image sensors, *Proc. IEEE Int. Conf. Comput. Vis.* 1 (2003) 122–129. <https://doi.org/10.1109/ICCV.2003.1238325>.
- [41] A. Beltran, V.L. Erickson, A.E. Cerpa, ThermoSense: Occupancy thermal based sensing for HVAC control, *BuildSys 2013 - Proc. 5th ACM Work. Embed. Syst. Energy-Efficient Build.* (2013). <https://doi.org/10.1145/2528282.2528301>.
- [42] T. Van Oosterhout, B. Kröse, G. Englebienne, People Counting with Stereo Cameras - Two Template-based Solutions, *VISAPP 2012 - Proc. Int. Conf. Comput. Vis. Theory Appl.* 2 (2012) 404–408. <https://doi.org/10.5220/0003865304040408>.
- [43] M. Aftab, C. Chen, C.K. Chau, T. Rahwan, Automatic HVAC control with real-time occupancy recognition and simulation-guided model predictive control in low-cost embedded system, *Energy Build.* 154 (2017) 141–156. <https://doi.org/10.1016/J.ENBUILD.2017.07.077>.
- [44] R. Rana, B. Kusy, R. Jurdak, J. Wall, W. Hu, Feasibility analysis of using humidex as an indoor thermal comfort predictor, *Energy Build.* 64 (2013) 17–25. <https://doi.org/10.1016/J.ENBUILD.2013.04.019>.
- [45] A. ANSI, M. Ashrae, Standard 55—thermal environmental conditions for human occupancy, *Amer. Soc. Heat, Refrig. Air Cond. Eng.* 1451992 (2017).

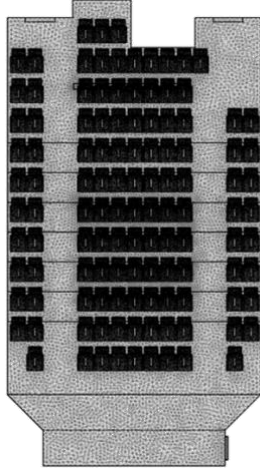
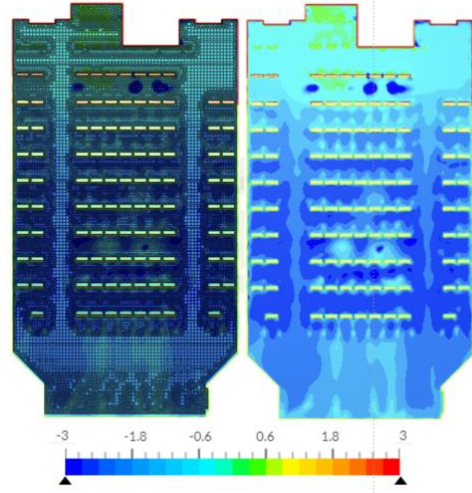
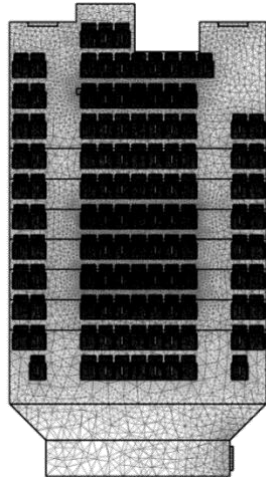
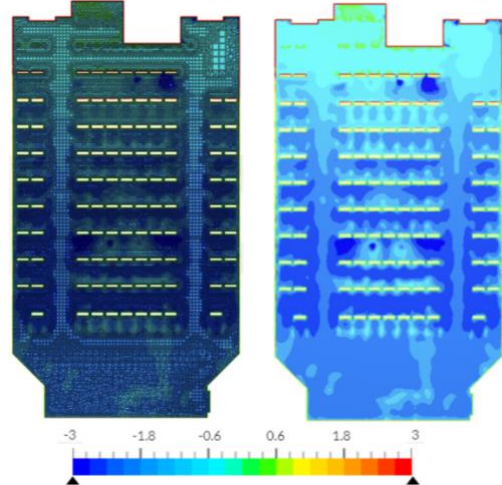
- [46] J. Van Hoof, Forty years of Fanger's model of thermal comfort: comfort for all?, *Indoor Air*. 18 (2008) 182–201. <https://doi.org/10.1111/J.1600-0668.2007.00516.X>.
- [47] P.O. Fanger, Thermal comfort. Analysis and applications in environmental engineering., *Therm. Comf. Anal. Appl. Environ. Eng.* (1970).
- [48] J. Murad, Harnessing the Power of the Cloud - Computational Fluid Dynamics With SimScale, *Am. Soc. Mech. Eng. Fluids Eng. Div. FEDSM*. 1 (2021). <https://doi.org/10.1115/FEDSM2021-66406>.
- [49] M. Popovac, K. Hanjalic, Compound wall treatment for RANS computation of complex turbulent flows and heat transfer, *Flow, Turbul. Combust.* 78 (2007) 177–202. <https://doi.org/10.1007/S10494-006-9067-X/METRICS>.
- [50] M. Breuer, N. Jovičić, K. Mazaev, Comparison of DES, RANS and LES for the separated flow around a flat plate at high incidence, *Int. J. Numer. Methods Fluids*. 41 (2003) 357–388. <https://doi.org/10.1002/FLD.445>.
- [51] M.F. R., Ten Years of Industrial Experience with the SST Turbulence Model, *Turbul. Heat Mass Transf.* 4 (2003) 625–632. <https://cir.nii.ac.jp/crid/1571135650766644352> (accessed January 26, 2023).
- [52] S.B. Heymsfield, B. Bourgeois, D.M. Thomas, Assessment of human energy exchange: historical overview, *Eur. J. Clin. Nutr.* 2017 713. 71 (2016) 294–300. <https://doi.org/10.1038/ejcn.2016.221>.
- [53] ultralytics/yolov5, (n.d.). <https://github.com/ultralytics/yolov5> (accessed January 30, 2023).
- [54] Classroom Monitoring Dataset | Kaggle, (n.d.). <https://www.kaggle.com/datasets/lunarwhite/classroom-monitoring-dataset> (accessed January 30, 2023).
- [55] J.Y. Shen, S. Kojima, X.Y. Ying, X.J. Hu, Influence Of Thermal Experience On Thermal Comfort In Naturally Conditioned University Classrooms, *Lowl. Technol. Int.* 21 (2019) 107–122. https://cot.unhas.ac.id/journals/index.php/ialt_lti/article/view/566 (accessed September 26, 2022).
- [56] G. Havenith, I. Holmér, K. Parsons, Personal factors in thermal comfort assessment: clothing properties and metabolic heat production, *Energy Build.* 34 (2002) 581–591. [https://doi.org/10.1016/S0378-7788\(02\)00008-7](https://doi.org/10.1016/S0378-7788(02)00008-7).
- [57] A.A. Bloutsos, P.C. Yannopoulos, Room Air-Conditioning Operating as a Filling Box, *Processes*. 10 (2022). <https://doi.org/10.3390/PR10020213>.
- [58] S. Clemente, S. Beauchêne, E. Nefzaoui, Generation of aggregated plug load profiles in office buildings, *Energy Build.* 252 (2021). <https://doi.org/10.1016/J.ENBUILD.2021.111398>.
- [59] Y. Acquaah, J.B. Steele, B. Gokaraju, R. Tesiero, G.H. Monty, Occupancy detection for smart hvac efficiency in building energy: A deep learning neural network framework using thermal imagery, *Proc. - Appl. Imag. Pattern Recognit. Work.* 2020-October (2020). <https://doi.org/10.1109/AIPR50011.2020.9425091>.
- [60] S. Karjalainen, Gender differences in thermal comfort and use of thermostats in everyday thermal environments, *Build. Environ.* 42 (2007) 1594–1603. <https://doi.org/10.1016/J.BUILDENV.2006.01.009>.

- [61] J. van Hoof, L. Schellen, V. Soebarto, J.K.W. Wong, J.K. Kazak, Ten questions concerning thermal comfort and ageing, *Build. Environ.* 120 (2017) 123–133. <https://doi.org/10.1016/J.BUILDENV.2017.05.008>.
- [62] H. Qin, X. Wang, A multi-discipline predictive intelligent control method for maintaining the thermal comfort on indoor environment, *Appl. Soft Comput.* 116 (2022) 108299. <https://doi.org/10.1016/J.ASOC.2021.108299>.
- [63] Z. Wang, J. Wang, Y. He, Y. Liu, B. Lin, T. Hong, Dimension analysis of subjective thermal comfort metrics based on ASHRAE Global Thermal Comfort Database using machine learning, *J. Build. Eng.* 29 (2020) 101120. <https://doi.org/10.1016/J.JOBE.2019.101120>.

Supplement materials

Table S1. Experimental results of mesh generation

Experiment 1			Mesh	Simulation (PMV)	Similarity
Basic setting	Algorithm: standard	Physics-based meshing: on			MRE=0.000 R ² =1.000
	Sizing: Automatic	Hex element core: on			
Statistics about mesh Quality	Finesse: 9/10 (Coarse to fine: 0~10)	Number of processors: 16			
	Overall mesh quality:	0.441 (Acceptable range: 0.035 to 1.0)			
	Number of volumes:	11,059,436			
	Number of prisms:	2,616,378			
	Number of triangles:	17,514,553			
	Number of faces:	25,238,234			
	Number of edges:	54,210			
	Number of hexahedra:	1,213,737			
	Number of pyramids:	314,870			
	Number of quadrangles:	7,723,681			
Time spending	Number of nodes:	4,041,116			
	Number of tetrahedra:	6,914,451			
	Meshing	63min			
	Simulation	206 min			
Experiment 2			Mesh diagram	Simulation (PMV)	Similarity
Basic setting	Algorithm: standard	Physics-based meshing: on			MRE=5.9% R ² =0.9524
	Sizing: Automatic	Hex element core: on			
Statistics about mesh Quality	Finesse: 7/10 (Coarse to fine: 0~10)	Number of processors: 16			
	Overall mesh quality:	0.351 (Acceptable range: 0.035 to 1.0)			
	Number of volumes:	6,184,244			
	Number of prisms:	1,377,399			
	Number of triangles:	8,931,297			
	Number of faces:	14,554,483			
	Number of edges:	44,695			
	Number of hexahedra:	1,146,419			
	Number of pyramids:	234,989			
	Number of quadrangles:	5,623,186			
Time spending	Number of nodes:	2,617,488			
	Number of tetrahedra:	3,425,437			
	Meshing	42 min			
	Simulation	91 min			

Experiment 3			Mesh diagram	Simulation (PMV)	Similarity
Basic setting	Algorithm: standard	Physics-based meshing: on			MRE=9.6% $R^2=0.8951$
	Sizing: Automatic	Hex element core: on			
Statistics about mesh Quality	Finesse: 5/10	Number of processors: 16			
	Coarse to fine (0~10)				
	Overall mesh quality:	0.257 (Acceptable range: 0.035 to 1.0)			
	Number of volumes:	5,028,507			
	Number of prisms:	994,105			
	Number of triangles:	8,851,520			
	Number of faces:	11,037,402			
	Number of edges:	43,229			
	Number of hexahedra:	192,861			
Time spending	Number of pyramids:	231,803			
	Number of quadrangles:	2,185,882			
	Number of nodes:	1,469,945			
	Number of tetrahedra:	3,609,738			
	Meshing	22min			
	Simulation	52 min			
Experiment 4			Algorithm	standard	Similarity
Basic setting	Algorithm: standard	Physics-based meshing: on			MRE=17.8% $R^2=0.8051$
	Sizing: Automatic	Hex element core: on			
Statistics about mesh Quality	Finesse: 3/10	Number of processors: 16			
	Coarse to fine (0~10)				
	Overall mesh quality:	0.201 (Acceptable range: 0.035 to 1.0)			
	Number of volumes:	4,878,610			
	Number of prisms:	973,889			
	Number of triangles:	8,712,551			
	Number of faces:	10,640,070			
	Number of edges:	42,924			
	Number of hexahedra:	118,103			
Time spending	Number of pyramids:	224,273			
	Number of quadrangles:	1,927,519			
	Number of nodes:	1,370,240			
	Number of tetrahedra:	1,370,240			
	Meshing	18 min			
	Simulation	41 min			

To assess the similarity between images, the simulation result graphs referred to in Table S1 are initially converted to a 32-bit floating-point data type with shape of (212*388*3). This data is subsequently transformed into grayscale value data (212*388*1) and ultimately reshaped into a strip format (82,256*1). The entire process is depicted in Figure S1. Using this data, the mean relative error (MRE) and the coefficient of determination (R^2) are calculated, with the respective formulas indicated as (S1) and (S2). The MRE value, which ranges from 0 to 1, signifies complete similarity at 0 and total dissimilarity at 1. As for R^2 , it has a range of 0 to 1, with values closer to 1 suggesting greater similarity between two figures. According to Table S1, all results are benchmarked against Experiment 1, which features the finest mesh quality (fineness =9) in this study.

$$MRE = 1/n * \sum_{i=1}^n \left(\frac{|I_1 - I_2|}{I_1} \right) \quad (S1)$$

$$R^2 = 1 - \frac{SSR}{SST} = 1 - \frac{\sum_{j=1}^n (I_1 - I_2)^2}{\sum_{j=1}^n (I_1 - \bar{I}_1)^2} \quad (S2)$$

where, I_1 and I_{12} represent the pixel values at corresponding positions in the two images, and n represents the total number of pixels.

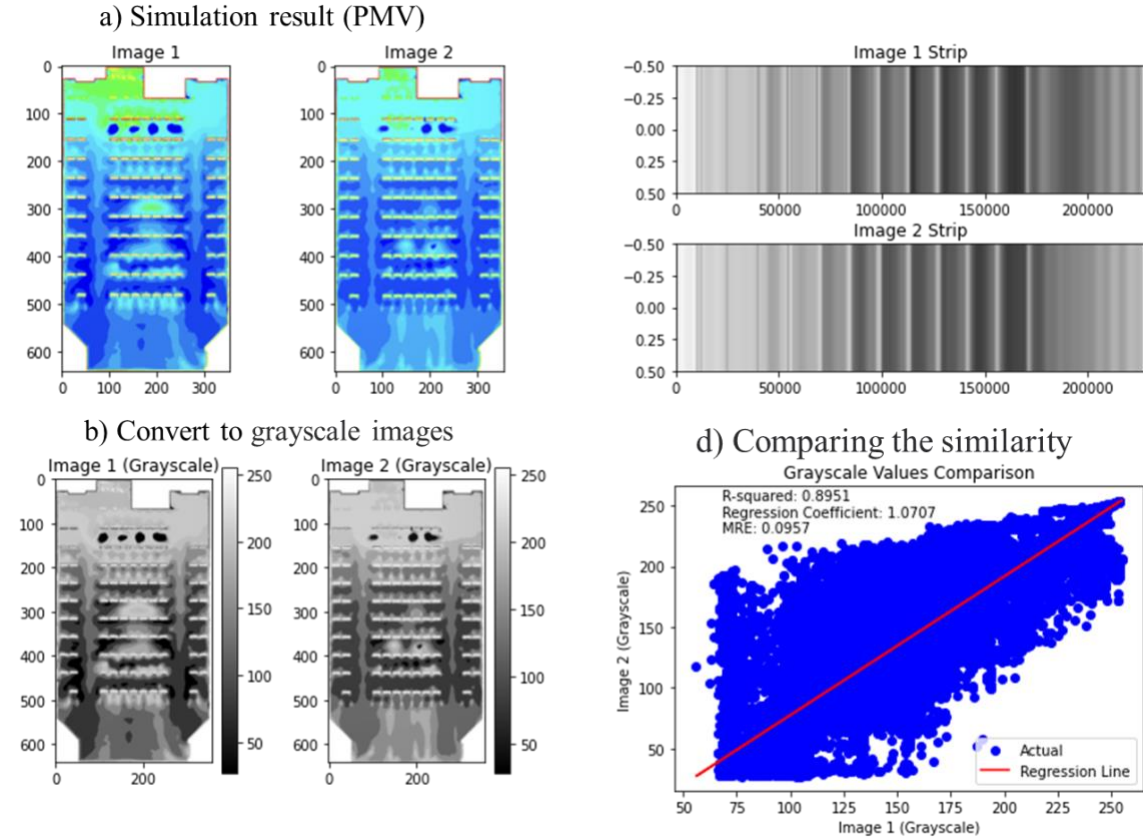


Figure S1. The process of comparing the similarity of the simulation result.